

A FORENSIC INVESTIGATION OF THE ELECTRICAL PROPERTIES OF
DIGITAL AUDIO RECORDING

by

JACK LEROI

B.S., Metropolitan State College, 2006

A thesis submitted to the
Faculty of the Graduate School of the
University of Colorado in partial fulfillment
of the requirements for the degree of
Master of Science
Recording Arts - Media Forensics

2014

© 2014

JACK LEROI

ALL RIGHTS RESERVED

This thesis for the Master of Science degree by

Jack LeRoi

has been approved for the

Recording Arts Program

by

Catalin Grigoras, Chair

Jeff Smith

Lorne Bregitzer

Date: May 2, 2014

LeRoi, Jack (M.S., Recording Arts - Media Forensics)

A Forensic Investigation of the Electrical Properties of Digital Audio Recording

Thesis directed by Associate Professor Catalin Grigoras.

ABSTRACT

In media forensics, the devices; e.g. computers, smart phones, still/video cameras, audio recorders, and software; e.g. video, audio, and graphics editors, file and disk utilities, mathematical computation applications, are, for the most part, black boxes. The design specifications are usually proprietary and the operating specifications may be incomplete, inaccurate, or unavailable. This makes it difficult to validate the technology, but using it without validation could discredit a practitioner's findings or testimony. The alternative is to test the device or program to determine relevant characteristics of its performance.

An important and common device in media forensics is the portable digital audio recorder used to record surveillance and interviews. This type can also be used to record the alternating current (AC) waveform from the mains power. While small variations in the AC frequency (ENF) can be forensically important, distortion in the recording can affect its value in adjudication or investigation. A method is presented to evaluate aspects of a recorder's operation that can cause distortion. Specifically, the method measures the noise generated by the recorder's electronics in its input and amplifier circuits. The method includes a procedure to isolate the recorder from environmental sources of noise. The method analyzes the broadband noise floor produced by the range of recording

conditions and recorder settings. It also analyzes the noise amplitude for the harmonics for the mains frequency.

The form and content of this abstract are approved. I recommend its publication.

Approved: Catalin Grigoras

TABLE OF CONTENTS

CHAPTER

I. INTRODUCTION.....	1
II. RATIONAL	6
III. PROCEDURES	8
IV. RESULTS.....	17
V. ANALYSIS.....	26
VI. CONCLUSION	30
REFERENCES.....	32

APPENDIX

A. ADDITIONAL NOISE LEVEL GRAPHS.....	34
B. ADDITIONAL HARMONIC LEVEL GRAPHS	40
C. EQUATIONS	65

CHAPTER I

INTRODUCTION

In a popular anecdote¹, the 3rd century BCE Greek scientist and mathematician Archimedes of Syracuse was asked by King Hieron II² to investigate whether the smith who had made the King's crown had substituted silver for some of the gold he was given. Archimedes was not allowed to melt the crown to compare its volume to that of the same weight in pure gold. He had to find a way, unknown at the time, to determine the volume of an irregularly shaped object. The solution came to him in his bath, as he observed the amount of water that his body displaced. Whether or not Archimedes then ran naked through the streets shouting "Eureka", Archimedes' principle explains the relationships among weight, density, and volume and is an important scientific discovery³.

However, while Archimedes' discovery is remarkable, in a larger sense, it is not exceptional. The observation and analysis of the physical world is a primary pursuit of *Homo sapiens*. From the earliest times, our survival, as creatures without fang or claw, depended on comprehending and manipulating nature. This ability of early humans to know and use the available materials, e.g. wood, stone, animal tissues, to understand weather and the plants and animals in their environment, was indispensable in the growth of culture and civilization.

Given these characteristics, and a human fossil record of 250,000 years⁴, modern science is a curiously late development. One can only speculate over the factors that prevented its earlier acceptance, but, paradoxically, the human need for explanation is a likely candidate. The naiveté of ancient peoples about causality left gaps in their phenomenology. In the absence of natural reasons for the world and its phenomena, they filled the gaps with their imagination. In their imagining, the world was animated by deities, spirits, and other intentional, but invisible beings.

Scientific methods depend on objective assessments of observable phenomena to produce natural explanations of those phenomena. Proof may be offered for natural explanations and such proof may either be accepted or rejected. Supernatural explanations are beyond proof and must either be believed or denied. The two types of explanations are incompatible. It cannot be that lightning is both a plasma discharge of differences in electrical potential and a thunderbolt thrown by Zeus from Mount Olympus. There cannot even be an intermediate explanation.

Supernatural explanations are appealing and emotionally satisfying in a way that natural explanations often are not. They are simple and inclusive and certain while natural explanations are complex, partial, provisional. They meet the human need for quick answers and risk avoidance that were inherited from our prey ancestors.

Science and technology are today so embedded in the physical and social culture of global civilization, that they supply the explanations and provisions that

formerly came from religion. They are so pervasive, it is impossible to experience the world the way it was before they existed, but, absent an alternative, rejecting supernatural explanations was likely very difficult. However, once agriculture and writing developed, people had the time and tools to investigate other possible reasons for the visible world. This fostered the ability to reason and laid the foundation for what later became the scientific method.

The curiosity that drives scientific exploration is an inherent human characteristic but the ways of thought it requires are not natural. Even those who have no supernatural beliefs are not therefore automatically scientific. The hardwired tendency, even need, to make quick decisions leaves us prone to logical fallacies and other mental errors. These errors are often embedded in heuristic methods like “common sense”. While common sense is often useful, the innate errors produce biases of various types. It is important to stress that these fallacies are not moral or intellectual failures but natural consequences of our neurology⁵. With this understanding, it is possible to mitigate the harmful effects of such fallacies.

It is instructive to consider the effect this tendency has had on forensic science. For many years, courts, law enforcement organizations, and even forensic practitioners themselves accepted the premise that every fingerprint was unique. This assumption was based on the experience of fingerprint examiners. Since identical fingerprints were never found, this uniqueness proposition was not disproved; therefore it was assumed that the lack of disproof amounted to

proof. (This is the “Argumentum ad Ignorantiam⁶”; i.e., “whatever is not false must be true, whatever is not true must be false.”)

Yet there is no known mechanism that would prevent prints from different fingers, either from the same or different persons, from being the same. As a result, it is impossible to use fingerprint evidence for positive identification⁷.

When Brandon Mayfield was arrested in 2004 for the Madrid bombings based on fingermarks that closely matched Ouhmane Daoud, it seemed that the uniqueness proposition was disproved. In fact, law enforcement had made an inaccurate identification. However, the issues raised by this case fit with the current movement in forensics towards scientific methods and away from heuristics. This trend was accelerated with the publication of the NAS report in 2009 that directly addresses the challenges in media forensics.

The developments in electronic technology in the last 100 years have produced a complex, bewildering, and ever changing technical environment. Since the invention of digital electronics, the worldwide saturation of millions of miniature recording devices has produced an overwhelming flood of image, video, and audio files. These have strained the ability of forensic practitioners to respond adequately to the demand. Given the limits on time, money, and personnel, it is tempting for them to accept categorically that their tools are adequate to the task. However, as with the uniqueness proposition, such acceptance is unwise, because, as with most end users, they typically have little or no knowledge about the inner workings of the technology on which they rely.

In particular, the operating characteristics of the hardware and software used in media forensics can be difficult to determine. Manufacturer's specifications may be missing or incomplete and the accuracy of the available information is not guaranteed. Failing to allow for this deficiency could discredit a practitioner's findings or testimony.

The better approach is to rigorously test technology to determine actual operation. These tests may cover the overall performance of a device or program, or may be focused on a specific factor or set of factors related to a particular application of the technology. Ideally, the results will show that the technology performs adequately for the intended task. If not, it must be rejected for that particular purpose, though it may yet be useful for others.

Guidelines for evaluating tools, techniques, and procedures are found in the "SWGDE Recommended Guidelines for Validation Testing", published by the Scientific Working Group on Digital Evidence.

CHAPTER II

RATIONAL

One of the applications of technology that is significant in media forensics is the capture and analysis of the fluctuations in the frequency of the electrical grid. For North America, the standard frequency is 60 Hz but this fluctuates as the aggregate load on the grid varies. As the load increases, the frequency sags until more power is added to the grid. As the load decreases, the frequency rises until power is removed from the grid. Since the load is constantly changing, the frequency is also constantly changing, though the power producers are required to hold the nominal frequency to 60 Hz ± 0.02 Hz⁸. (The actual frequency may vary up to ± 0.05 Hz before the system is considered over limit⁹.) Because the variations are non-cyclical (non-deterministic), the actual frequencies that occur between any two moments cannot be predicted or modeled. Thus, the sequence of frequencies between those two moments can provide a timestamp that indicates when that sequence of frequencies occurred.

The variations in the Electric Network Frequency (ENF) can be acquired unintentionally during the recording of audio signals¹⁰. This occurs in a number of ways. For one, when an electromagnetic field is generated by the electric current flowing in the grid, the field can induce an ENF signal into the recorder's microphones or into its audio amplifier circuits. This signal is combined with the intended audio signal. For another, the recorder can receive an ENF signal

through an external (mains) power supply. If the 60 Hz AC from the mains is not adequately filtered from the DC power supply, an ENF signal can be induced in the recorder's audio amplifier circuits. Again, this signal is combined with the intended audio signal.

The variations in the Electric Network Frequency (ENF) can also be acquired deliberately. In order to use a recording of an unknown sequence of ENF variations as a timestamp, there must be a known sequence of ENF variations to compare it to. To this end, databases of the ENF are acquired and maintained for each electrical grid¹¹. The house voltage from the mains is converted to audio levels and applied to the audio inputs of the recording device used for the database.

The utility of this method depends on the accuracy and precision with which the ENF is recorded. The discrepancy between the original signal and a recording of it are classified as acquisition errors. These errors are generated at different stages in the circuitry of the recording device; the way and extent to which these errors affect the recorded ENF signal determine whether it can be used to validate the time of a recording. This paper describes some of the factors of digital recording that can lead to these acquisition errors.

CHAPTER III

PROCEDURES

The initial investigation of a recording device requires the evaluation of its noise characteristics. This evaluation should measure the random fluctuations in electrical potential produced in the input and processing circuits of the device. The factors contributing to the noise figure are internal sources of noise as well as noise that arises from the environment in which a recording is made.

Internal sources include thermal noise, shot noise, and flicker noise. These are generated by the recorder's electronic components themselves¹².

Environmental sources include atmospheric¹³ and industrial noise¹⁴. These are generated by lightning and by discharges of electrical energy by machinery and electrical devices. The sudden change in electrical potential generates electro-magnetic fields which induce noise in the recorder's electronic components.

Fluctuations in electrical potential can also be induced in the device's components by other environmental phenomena. The most significant phenomena are the electro-magnetic fields produced by current flowing in the electric power network. The fluctuations in these fields are not random. The variations in strength are synchronous with the amplitude and frequency of the sine wave driving the electrical grid. The fluctuations may be recorded as hum at the electric network frequency, 60 hertz for North America.

In a digital recorder, there is also noise added to the signal by the Analog-to-Digital conversion. This noise is caused by quantization error in the ADC and jitter in the sampling clock.

To properly evaluate a recorder's noise figure, it is necessary to eliminate all influence by environmental sources. This may be accomplished in one of two ways. Either the recorder can be located in an area where these fields are absent or the recorder can be shielded from whatever fields are present. It is possible to eliminate industrial noise and hum by locating the recorder away from all electric power system components, machinery, and electrical devices, but this will not eliminate atmospheric noise. However, the use of proper shielding will reduce all ambient fields to insignificant levels.

The procedures for this paper were developed using the facilities of the National Center for Media Forensics. The equipment included a Stanford Research Systems SR770 FFT spectrum analyzer, a Ramsey Electronics STE3000FAV faraday shielded enclosure, and an Olympus DM-520 battery powered portable digital audio recorder. The SR770 contains a low distortion sine wave generator.

Since the STE3000FAV is designed to block cell phone signals in the 20 megahertz to 8 gigahertz range, it was necessary to validate the enclosure's performance in the audio range, particularly at the electric network frequency of 60 hertz. The complication in performing this validation was the lack of a calibrated test instrument. As a substitute, a portable recorder was used to receive any electro-magnetic energy in the audio range that leaked through the

shielding. However, this was bootstrapping because the very object of these procedures was to evaluate the recorder. The workaround was finally accomplished by adding an initial step. In this first step, the recorder was used in an environment that was free of electro-magnetic fields. (Note that it was impossible to accomplish the entire procedure in this environment because of the need for mains power for the SR770.) The field free recordings were analyzed for periodic phenomena. Due to the absence of external electro-magnetic fields, any phenomena must have been generated by the recorder itself. These results were then used to calibrate the recordings made with the DM-520 placed in the STE3000FAV in the lab.

Recordings were made with the DM-520 in the STE3000FAV, with the lid closed and latched. This provided the maximum electro-magnetic isolation. However, in this configuration there is no way to apply an external signal to the DM-520. Leaving the lid unlatched and slightly open allowed connecting a thin audio cable between the SR770 signal generator and the DM-520, but this spoils the integrity of the enclosure. It was necessary to determine whether recordings made with the configuration showed increased levels of environmental noise. To this end, recordings were made with an audio cable connected to the signal generator output of the SR770. It was run underneath the lid of the STE3000FAV and the audio plug at the end of the cable was placed near the input jack of the DM-520, but not connected to it.

The DM-520 has 16 recording levels, 3 input gain levels, and 2 sampling rates, resulting in 96 unique settings. There were also 2 recording environments,

field and lab. The field tests had 1 input state, shorted. The lab tests had 2 input states, shorted and open. The lab test also had 2 recording conditions, shielded and partially shielded. Testing all of these combinations would require 480 recordings; however, evaluating the DM-520's noise performance only required testing a representative sample of these settings. The recording levels were reduced to half by selecting every other one, resulting in 240 combinations for testing. The reduction halved the work effort required to collect and process the recordings. Practically, the results for the missing combinations can be extrapolated from these 240 combinations.

The input circuits of an audio recorder amplify the electrical signals from a microphone or external audio source. These circuits produce internal noise from the activity of the electrons that flow through them. This activity can be influenced by the impedance of the microphone or external audio source. By testing the DM520 with the input shorted and with the input open, the impedance applied to the input circuits is either 0 ohms or infinite ohms. These two states provide the bounds for the impedance of anything connected to the recorder. The output impedance of the SR770 signal generator is specified as less than 5 ohms, so the self generated noise of the DM520's input circuits with the SR770 connected is near the results obtained with a shorted input.

The device to encode a continuously variable voltage (analog) to a series of fixed binary values (digital) is called an Analog to Digital convertor. Such a convertor is at the heart of every digital audio recorder. To complete a conversion, the changing analog voltage must be fixed at a static level long

enough for it to be encoded into a digital value. This is done by a sample and hold circuit that freezes the voltage until the conversion is complete. The time for this conversion must be sufficiently short to fit within the time window between samples. The time to charge the sample and hold circuit must also fit in the window before the conversion time.

In a digital audio recorder, noise is also generated in the Analog to Digital Converter (ADC). One source of this ADC noise is non-linearity in its transition levels. Figure 3.1 shows the relationship between an analog input and the digital output for a 3 bit ADC.

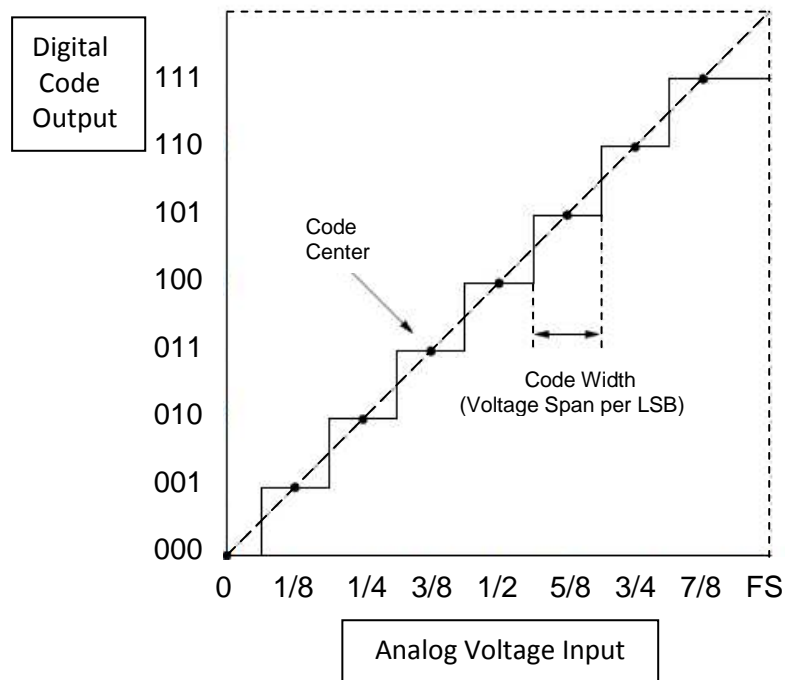


Figure 3.1

As the voltage increases or decreases, the code changes when the voltage crosses the transition point between one code and the one adjacent. If the voltage difference between transition points varies, then the response of the ADC is non-linear. This non-linearity produces noise in the digital output.

It is possible to measure the non-linearity of an ADC by applying a waveform of known probability density to its voltage input and analyzing the code output¹⁵. The voltage range of the input signal should cover the transition points of interest. During the design and testing of ADC components, the voltage range of the signal covers the entire input range of the ADC. For the purposes of this investigation, the transition points of special interest are around the 0 voltage point. Any non-linearity in this area can affect the accuracy and precision of zero crossing measurements of the ENF. This is of particular importance in using the recordings in ENF databases.

Three common waveforms used for testing are the saw tooth, triangle, and sine. The saw tooth and triangle waveforms are the easiest to compute from since they are theoretically linear, that is they have the same change in voltage per unit time. Thus they have an equal probability for each transition point. However, it is difficult to generate these as truly linear and the equipment to generate them is uncommon. However, high quality sine wave generators are readily available and, while the probability density computations are more complicated than those for linear waveforms, this is the standard approach.

For an ideal ADC, the distribution of digital code values matches the distribution of voltage values in the input waveform. Any non-linearity shows as differences in the distribution. However, using probability to measure non-linearity requires the acquisition of large data sets. This is because the infinite voltage values in the input have to be captured in the finite number of code output values. (These code values are also sometimes called “buckets”.) In

addition, any random noise in the input will be reduced, as large data sets average the input variations.

Field Noise Recording Procedure

Settings.

Recorder: Olympus DM-520

Serial Number: 100104915

Bit Depth: 16

Sampling Rate: 44.1 kHz, 48 kHz

Input: External Microphone

Input State: Shorted

Microphone Sensitivity: Low/Medium/High

Recording Levels: 2, 4, 6, 8, 10, 12, 14, 16

Step 1.

Insert the shorted plug into the external microphone jack.

Step 2.

Record samples approximately 36 seconds long.

@ 2 sampling rates

@ 3 microphone sensitivities

@ 8 recording levels

@ 1 input state

48 Samples Total

Step 3.

Trim the sample files to 30 seconds.

Save the trimmed samples to wave files.

Step 4.

Plot the waveform for each wave file created in Step 3.

Save the graph for each waveform plot.

Step 5.

Calculate the long term spectrum (Fourier transform) for each wave file created in Step 3.

Plot each long term spectrum.

Save the graph for each long term spectrum plot.

Lab Noise Recording Procedure

Settings.

Recorder: Olympus DM-520

Bit Depth: 16

Sampling Rate: 44.1 kHz, 48 kHz

Input: External Microphone

Input State: Shorted, Open

Microphone Sensitivity: Low/Medium/High

Recording Levels: 2, 4, 6, 8, 10, 12, 14, 16

Step 1.

Insert the shorted/open plug into the external microphone jack.

Step 2.

Record samples approximately 36 seconds long.

@ 2 sampling rates

@ 3 microphone sensitivities

@ 8 recording levels

@ 2 input states

@ 2 recording conditions

192 Samples Total

Step 3.

Trim the sample files to 30 seconds.

Save the trimmed samples to wave files.

Step 4.

Plot the waveform for each wave file created in Step 3.

Save the graph for each waveform plot.

Step 5.

Calculate the long term spectrum (Fourier transform) for each wave file
created in Step 3.

Plot each long term spectrum.

Save the graph for each long term spectrum plot.

CHAPTER IV

RESULTS

The use of digital audio recording is common in forensics. Recordings are created during surveillance and interviews, and are used in investigations and as evidence in legal proceedings. The noise measurements made for this paper provide the basis for choosing recording settings that have the least noise and highest fidelity.

The first selection to consider is the sampling rate. For the DM-520, the choice is between 44.1 kHz and 48 kHz. In the 240 sample files, there are 120 pairs of files whose settings differ only by their sampling rate. Figure 4.1 displays the comparison between the 44.1 kHz and 48 kHz sample files for the field recordings set for medium microphone sensitivity and recording level 8. The input was shorted.

The 4 plots display the graphs of the Fourier Transforms for the 2 sample files. The 44.1 kHz file is on the left; the 48 kHz file is on the right. The upper plots are the left channels; the lower plots are the right channels. The frequency range of the X axis is from 0 Hz (not including the DC component) to 20 kHz, inclusive. The bin width, or resolution, is 0.033333333333333 Hz. The decibel range of the Y axis is from -180 to -70. 0 DB is referenced to a full scale output of the 16 bit ADC, which is $2^{15} - 1$. The green line on each plot is the mean value of the channel samples.

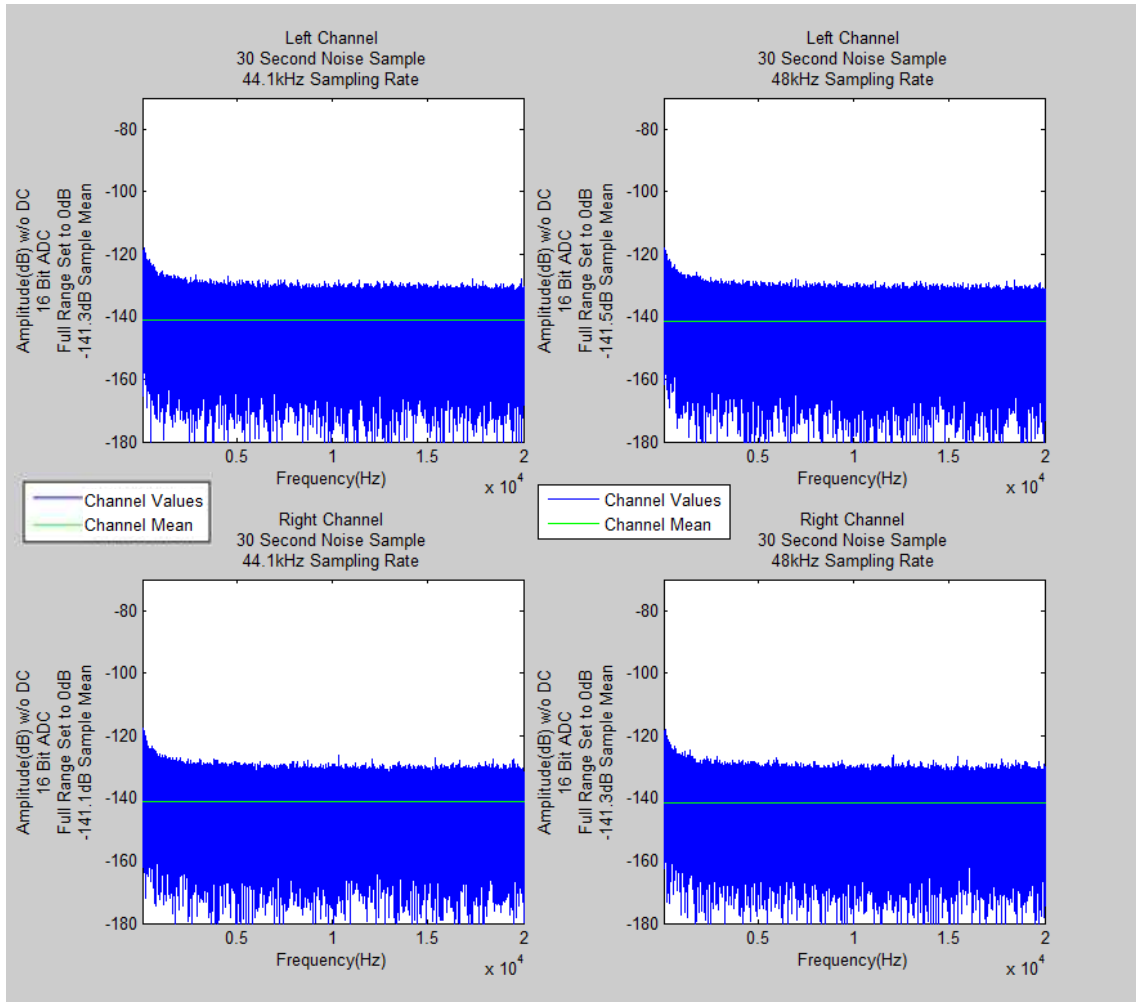


Figure 4.1
DM-520 – 30 Second Field Noise Test
Shorted Input, 16 Bit
Medium Microphone Sensitivity, Recording Level 8

Comparing the mean values for the corresponding channels in Figure 4.1 supplies a measure of the relative amounts of noise in the channels. This is justified by the similar contours of the FFT plots. For these two recordings, the difference for both channels is the same at 0.2 decibels. Comparing the mean values for all the corresponding channels will show any relationship between noise and sample rate.

Figure 4.2 displays the graphs of the differences between the mean values for all the corresponding channels in the 240 sample files.

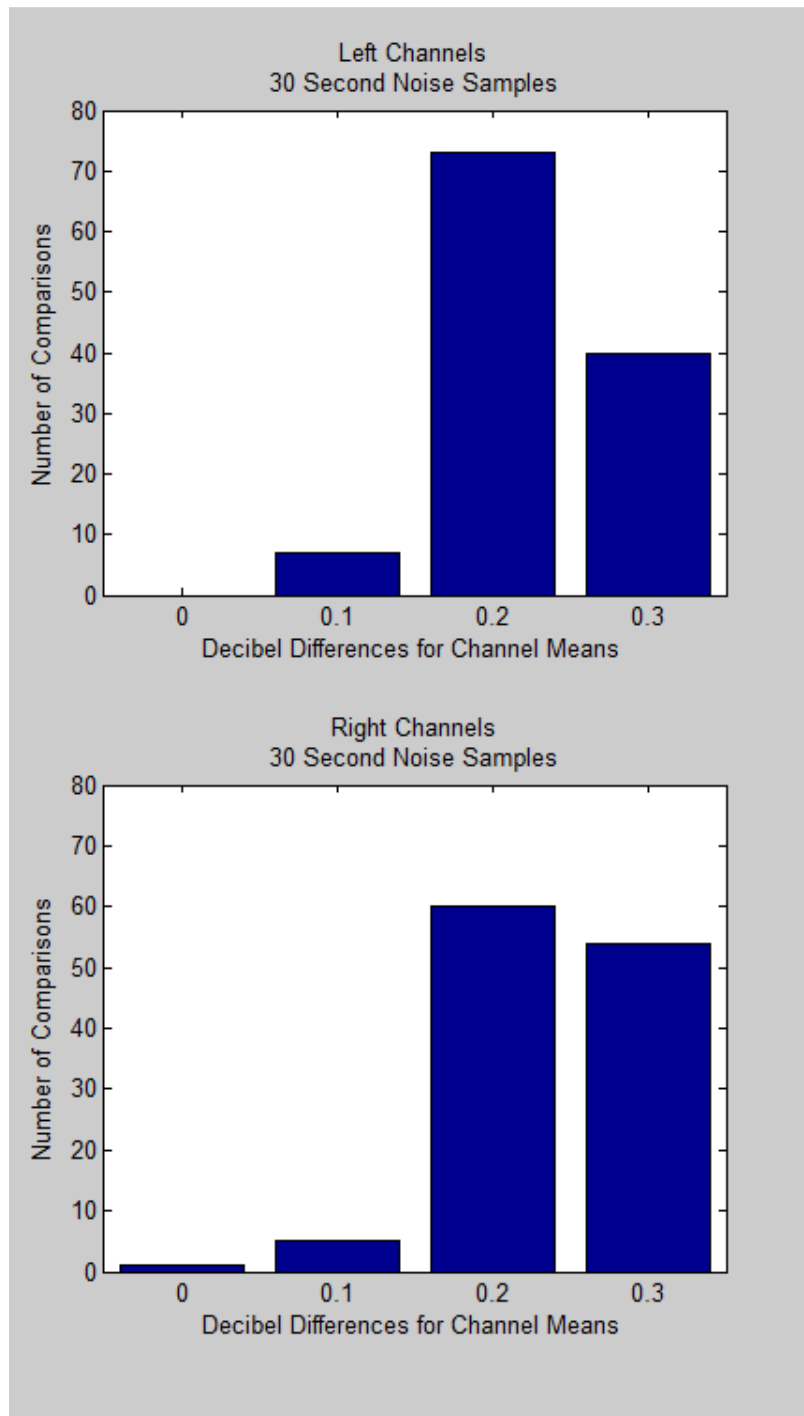


Figure 4.2
DM-520 – 30 Second Noise Tests
Corresponding Channel Comparisons

The histogram shows the distribution of the differences between the sample means for the left and right channels. The greatest difference between any 2 corresponding channels is 0.3 decibels. (The values for the sample means are rounded to 1 decimal place.)

Figure 4.3 displays the graph for the sample means for all 240 sample files. For this graph, the mean values for the 2 channels in each sample file are averaged. This is justified because the maximum difference for the channels for any sample file is less than 0.21 decibels. Table 4.1 shows the key for the recording parameters for the files whose means are displayed in Figure 4.3.

Table 4.1
DM-520 – 30 Second Noise Tests
Recording Conditions

Zone	Sampling Rate	Recording Location	Shielding	Input
1 - Left	44.1 kHz	Field	None	Shorted
1 - Right	48 kHz	Field	None	Shorted
2 - Left	44.1 kHz	Lab	Full	Shorted
2 - Right	48 kHz	Lab	Full	Shorted
3 - Left	44.1 kHz	Lab	Full	Open
3 - Right	48 kHz	Lab	Full	Open
4 - Left	44.1 kHz	Lab	Partial	Shorted
4 - Right	48 kHz	Lab	Partial	Shorted
5 - Left	44.1 kHz	Lab	Partial	Open
5 - Right	48 kHz	Lab	Partial	Open

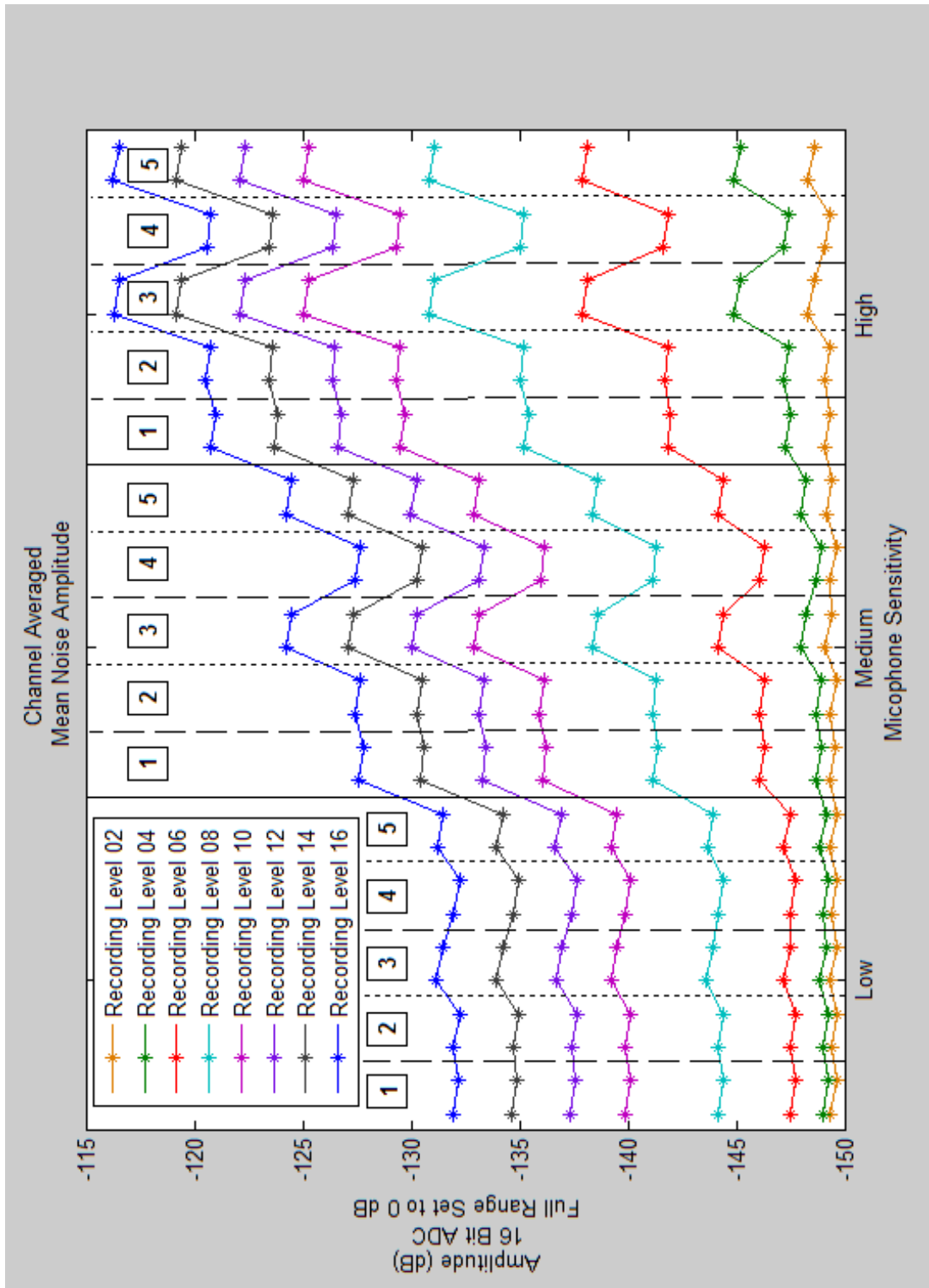


Figure 4.3
DM-520 – 30 Second Noise Tests
Channel Averaged
Mean Noise Amplitude

The graph is divided into 3 areas according to the microphone sensitivity setting when the recordings were made. Each area is divided into 5 zones. Each zone number has the same set of recording conditions as shown in Table 4.1. The value on the left side of each zone is for a 44.1 kHz sampling rate. The value on the right side of each zone is for a 48 kHz sampling rate.

It is also useful to look at the results aggregated by recording level. Figure 4.4 displays the relative noise figures for the 24 field recordings made at the 48 kHz sampling rate. From this graph, noise figures can be estimated for the recording levels that were not tested. The complete set of 10 graphs is included in Appendix A.

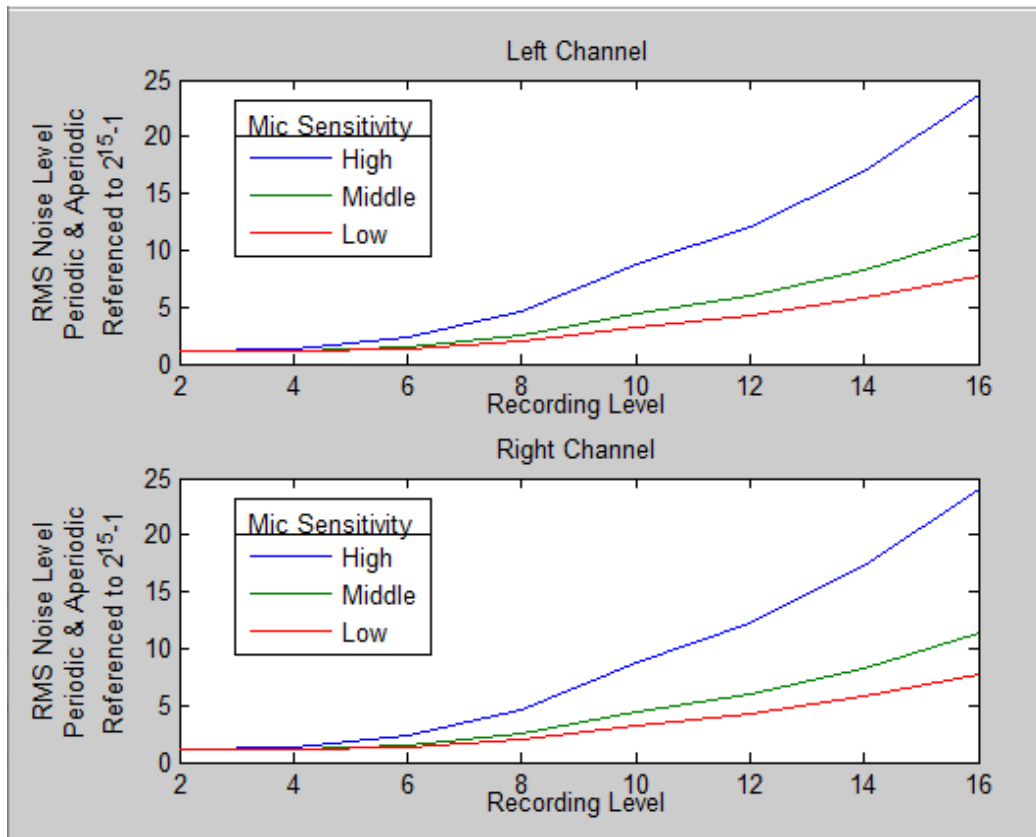


Figure 4.4
DM520 – 30 Second Field Noise Tests
Shorted Input, 48k Sampling Rate, 16 Bit

Besides addressing a recorder's broad band noise performance, the methodology being advocated here should also account for noise in the narrow band around the mains frequency (ENF) and its upper harmonics. For this evaluation, the ENF is 60 Hz. The first 7 upper harmonics are also included, from 120 to 480 Hz.

Figure 4.5 displays the 48 kHz sample file for the field recording with settings for medium microphone sensitivity and recording level 8. The input was shorted. The 4 plots display the graphs of the Fourier Transforms for the sample file. The upper plots are the left channel; the lower plots are the right channel. The full range FFT is on the left. The frequency range of the X axis is from 0 Hz (not including the DC component) to 20 kHz, inclusive. The bin width, or resolution, is 0.0333333333333333 Hz. The decibel range of the Y axis is from -180 to -70. 0 DB is referenced to a full scale output of the 16 bit ADC, which is $2^{15} - 1$. The amplitudes of the 60 Hz component and its upper harmonics are on the right. The green line on each plot is the mean value of the channel samples.

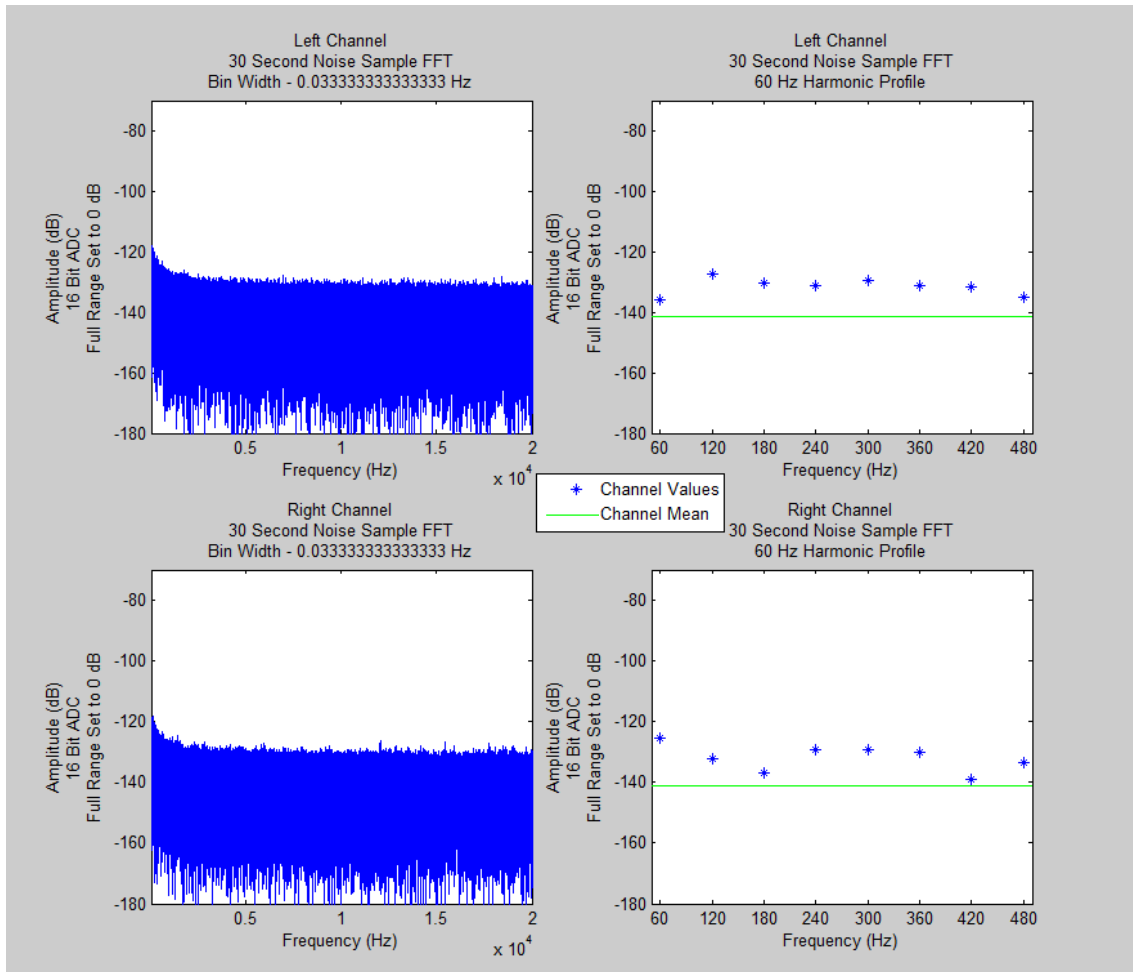


Figure 4.5
DM-520 – 30 Second Field Noise Test
Shorted Input, 48k Sampling Rate, 16 Bit
Medium Microphone Sensitivity, Recording Level 8

Figure 4.6 displays the aggregate for the 10 sample files recorded with medium microphone sensitivity at recording level 8. The complete set of 24 graphs is included in Appendix B.

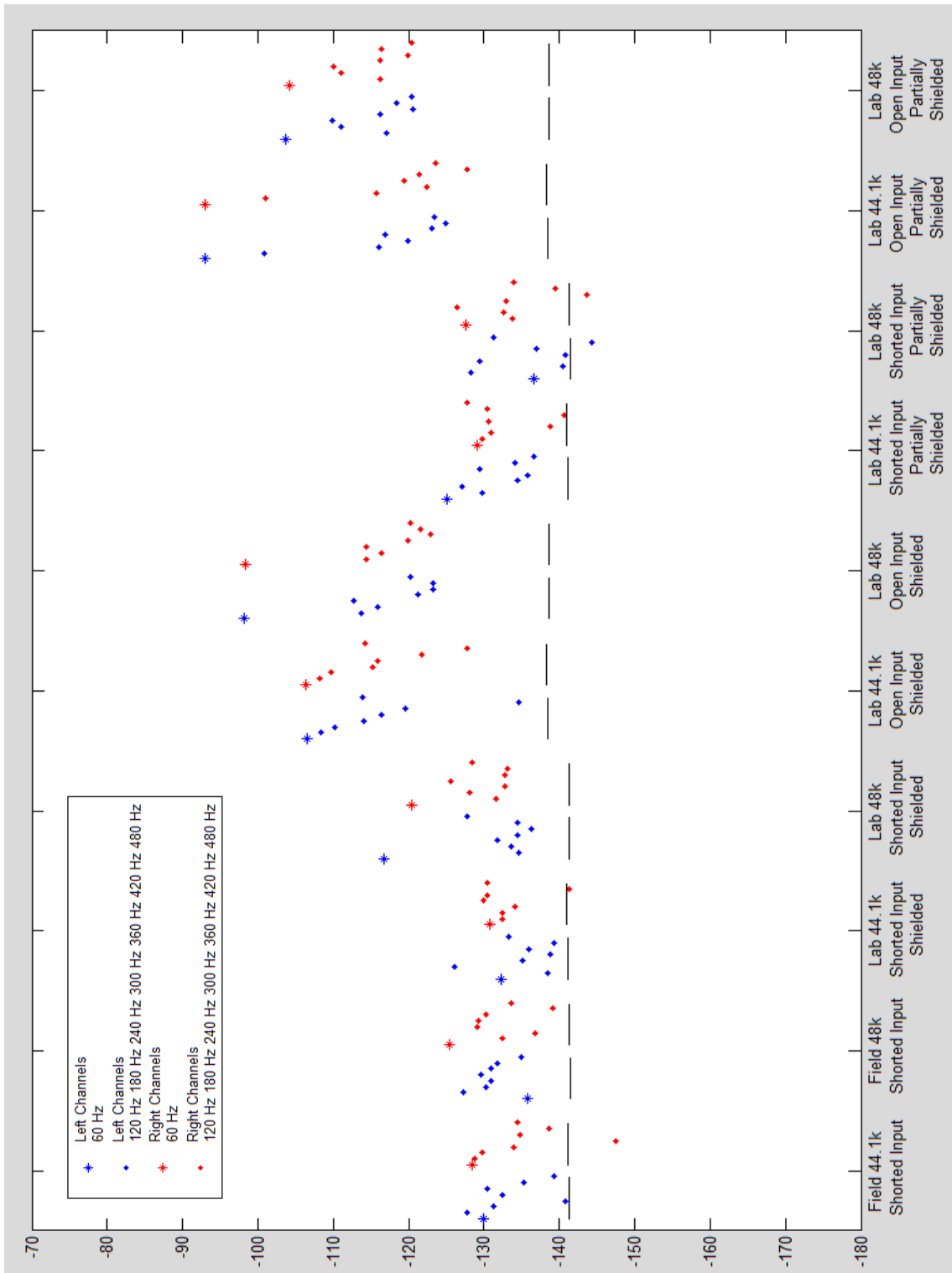


Figure 4.6
DM520 – 30 Second Lab Noise Tests
60 Hz Harmonic Levels
Medium Microphone Sensitivity, Recording Level 8

CHAPTER V

ANALYSIS

In Figure 4.2, the histogram shows that the greatest difference between the sample means for any corresponding right or left channels in the 204 sample files is 0.3 decibels. The code that produced the graph measures only the absolute difference between the sample means. It does not track whether the mean value is greater for the channel in the 44.1 kHz or the 48 kHz file. This information is lost when the results are aggregated. From this graph, it appears that there is no significant difference in internal noise generated by the 2 different sampling rates.

However, a pattern does emerge when the sample means are graphed sequentially. In Figure 4.3, the left points in each zone are the sample means for the 44.1 kHz file for each recording level. The corresponding right points are the sample means for the 48 kHz file for the recording level. It is clear from the graph that the 48 kHz sampling rate produces a slight but consistent difference from the 44.1 kHz rate. This appears to be a computational artifact due to the difference in the bandwidths for the 2 sampling rates. (The equations are given in Appendix C.)

The 48 kHz sampling rate has an upper frequency limit (Nyquist frequency¹⁶) of 24 kHz. This is 1.95 kHz higher than the upper frequency limit of the 44.1 kHz sampling rate. (The graphs in Figure 4.1 are by convention

restricted to the audio range of 20 Hz to 20 kHz so the additional bandwidth for the 48 kHz sample file is not visible.)

Assuming that the upper frequency limit of the anti-aliasing is raised a corresponding amount, and assuming that the noise generated in the recorder's input has power in that additional range, there should be a wider noise spectrum for the 48 kHz sample rate. If the long term spectrum for both sampling rates were flat, the sample means should be equal. However, the slope of the LTS for both sampling rates declines at the higher frequencies.

Including the higher frequencies in the mean likely produces a lower value for the wider spectrum of the 48 kHz files. (The Further calculations would show whether restricting averaging to the audio range would eliminate this consistent difference. In either case, the difference is minor and is unlikely to have much significance.

While the choice of sampling rate has little apparent influence on the amount of noise in the consequent recording, other settings and conditions have a much greater effect. These effects can be deduced from the graphs in Figures 4.3 and 4.4. It should be noted that the most striking aspect of Figure 4.3 is the consistency in the profiles of the plot lines.

As might be expected, increasing the sensitivity (gain) of the microphone preamp increases the amount of noise in the recording. The amount of noise also increases with higher recording levels. In addition, it is discernible that for each recording level in each microphone sensitivity area, there are two correlations among the file types. The noise figures for sample files made with

the same sampling rate and shorted inputs are the same, as are the noise figures for those with open inputs. It is clear that the noise figures for the files with open inputs are significantly higher than for those with shorted inputs. The greatest difference, however, is only 5 dB. Overall, the broadband noise performance of the DM-520 is excellent considering that the greatest mean value is approximately -178 dB below full range.

An issue not addressed by the previous analyses is the possible presence of tones at frequencies that interfere with the accidental or deliberate acquisition of the ENF. The following analysis speaks to this issue.

In North America, the ENF is 60 Hz, ± 0.02 Hz. When the ENF is recorded, any periodic noise at this frequency or its upper harmonics will interfere with measuring the actual ENF. Figure 4.5 displays the 48 kHz sample file for the field recording set for medium microphone sensitivity and recording level 8. The input was shorted.

The 60 Hz harmonic profiles in Figure 4.5 are within the noise band for both channels. There is no evidence of periodic noise at any of the frequencies.

The same analysis was performed for the rest of the 240 sample files. The results were aggregated by microphone sensitivity and recording level. Figure 4.6 displays the results for medium microphone sensitivity and recording level 8. As with the sample means for the wide band spectra shown in Figure 4.3, the harmonic content is greater for the files with open inputs. The values for the harmonic frequencies are generally higher than the channel mean. This is partly a statistical variation due to the random nature of the noise and partly a result of

the low frequency emphasis in the analog to digital conversion process. Since these samples are relatively short at 30 seconds, using a longer sample should reduce the variation from sample file to sample file at the same harmonic frequency. It should also reduce the variation among different harmonic frequencies in the same file.

CHAPTER VI

CONCLUSION

This document has presented a methodology for evaluating some aspects of the performance of a single unit of one type of portable digital recorder. The results obtained here would be useful in judging whether the performance of this unit is adequate to allow a valid measurement of the fluctuations in the ENF recorded by it. Yet, the results do not cover all the aspects of the recorder's performance that might introduce errors during the acquisition of the ENF. The methodology as developed so far concentrates on the performance of the audio input circuits. The next step is to measure the performance of the ADC in the unit, in particular its linearity, using a waveform of known probability density. This analysis is usually done during the design of an ADC where other sources of noise can be minimized. In this case, it is an open question whether the noise from any non-linearity can be separated from that from other sources. Further testing is necessary to determine whether it can be done successfully.

It is important to note that while the methodology may be valid for other models of recorder, these results and analyses are not. They do not even apply to other units of the same model. In order to be valid for any particular device, they must be done on that unit. To do otherwise is not only foolish; it is at least intellectually dishonest.

It is also important to consider that the most important part of this or any other methodology is not the methodology itself. Technology changes; understanding and knowledge increase; methodologies must develop to stay relevant. The most important part is the skepticism that drives it. Answers and conclusions are always partial and conditional. Continually questioning what is known and what is believed is the antidote for false assumptions and lax attitudes. By not blindly accepting the status quo and looking at things from more than one perspective, it is possible to find hidden connections and reveal problems that would otherwise go undetected. This effort is crucial to sustain and enhance the usefulness and validity of forensic science in all its disciplines.

REFERENCES

1. Heath, T.L. *The Works of Archimedes*. Cambridge: The University Press, 1897. xix. Print.
2. "Hieron II." *Encyclopaedia Britannica*. Encyclopaedia Britannica, Inc., 2014. Web. 22 Apr. 2014.
3. Heath, T.L. *The Works of Archimedes*. Cambridge: The University Press, 1897. 257. Print.
4. "Human Evolution >> Dating." *What does it mean to be human?* Smithsonian Institution, 2014. Web. 22 Apr. 2014.
5. Dror, Itiel E., and David Charlton. "Why Experts Make Errors." *Journal of Forensic Identification*. 56.4 (2006): 612. Print.
6. "Argumentum ad Ignorantiam." *Philosophy103: Introduction to Logic*. Lander University, 2004-9. Web. 29 Apr. 2014
7. The Fingerprint Inquiry. *The Fingerprint Inquiry Report*. Edinburgh, Scotland. 2011. 740. Print.
8. North American Electric Reliability Corporation. *Standard BAL-004-0 Time Error Correction*. 1 Apr. 2005. 1, Print.
9. NERC Balancing Authority Controls Standard Drafting Team. *Time Error Correction*. 2. Print.
10. Grigoras, C. "Applications of ENF Analysis in Forensic Authentication of Digital and Video Recordings." *Journal of Audio Engineering Society*. 57.9 (2009): 643-661. Print.
11. Grigoras, C., Jeff Smith, and Chris Jenkins. "Advances in ENF Database Configuration for Forensic Authentication of Digital Media." *Proceedings of the 131st Convention of the Audio Engineering Society*. Print.
12. Van Der Ziel, A. "Noise in Solid-State Devices and Lasers." *Proceedings of the IEEE*. 58.8 (1970). Print.

13. Furutsu, K., and T. Ishida. "On the Theory of Amplitude Distribution of Impulsive Random Noise." *Journal of Applied Physics*. 32.7 (1961): 1206-1221. Print.
14. Bell, L. H., and Douglas H. Bell. *Industrial Noise Control: Fundamentals and Applications*. CRC Press, 1993. Print.
15. Doernberg, J., Hae-Seung Lee, and David A. Hodges. "Full-Speed Testing of A/D Converters." *IEEE Journal of Solid-State Circuits*. SC-19.6 (1984): 820-827. Print.
16. Pohlmann, Ken C. *Principles of Digital Audio*. New York: McGraw-Hill, 2005. 25. Print.

APPENDIX A
ADDITIONAL NOISE LEVEL GRAPHS

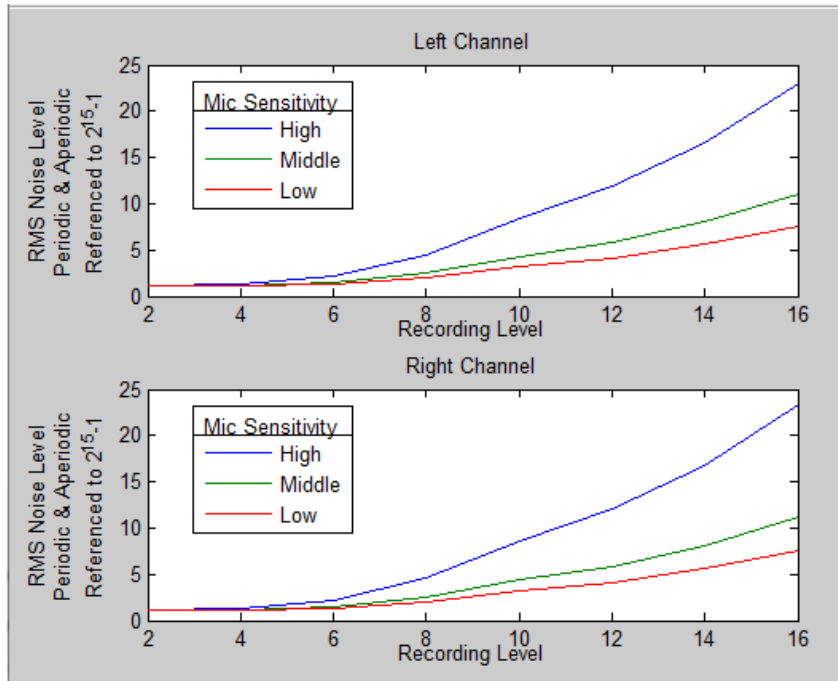


Figure A.1
DM520 – 30 Second Field Noise Test
Shorted Input, 44.1k Sampling Rate, 16 Bit

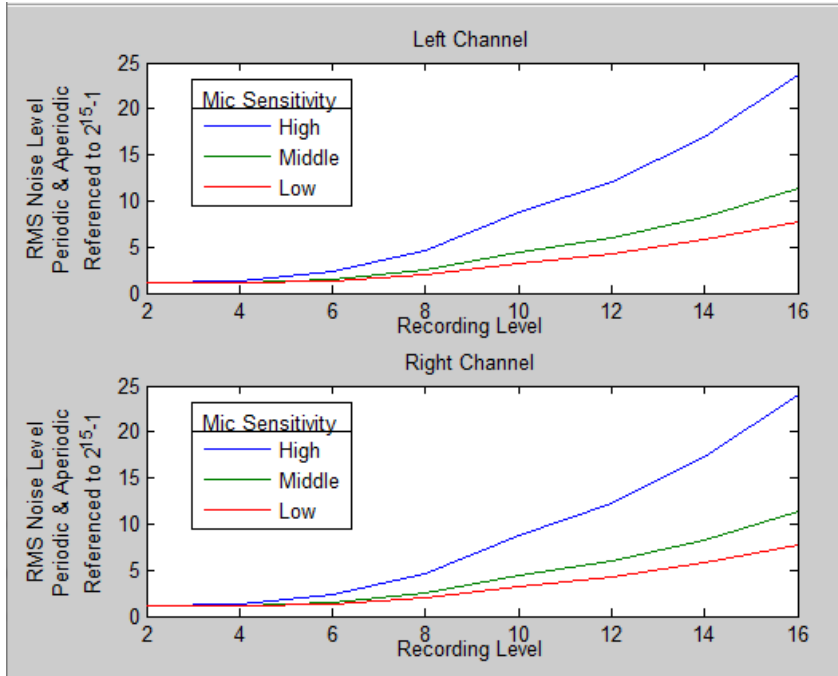


Figure A.2
DM520 – 30 Second Field Noise Test
Shorted Input, 48k Sampling Rate, 16 Bit

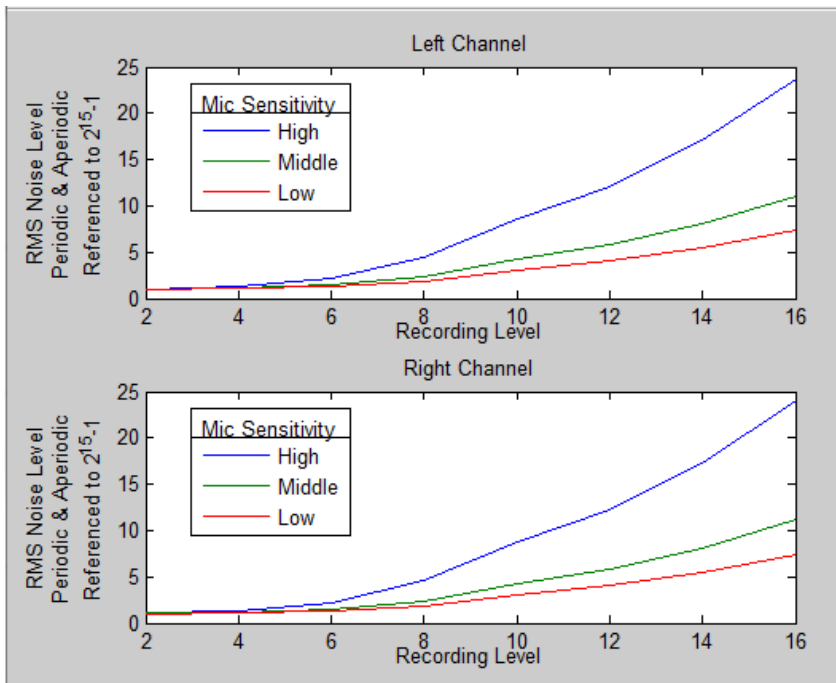


Figure A.3
DM520 – 30 Second Lab Noise Test, Fully Shielded
Shorted Input, 44.1k Sampling Rate, 16 Bit

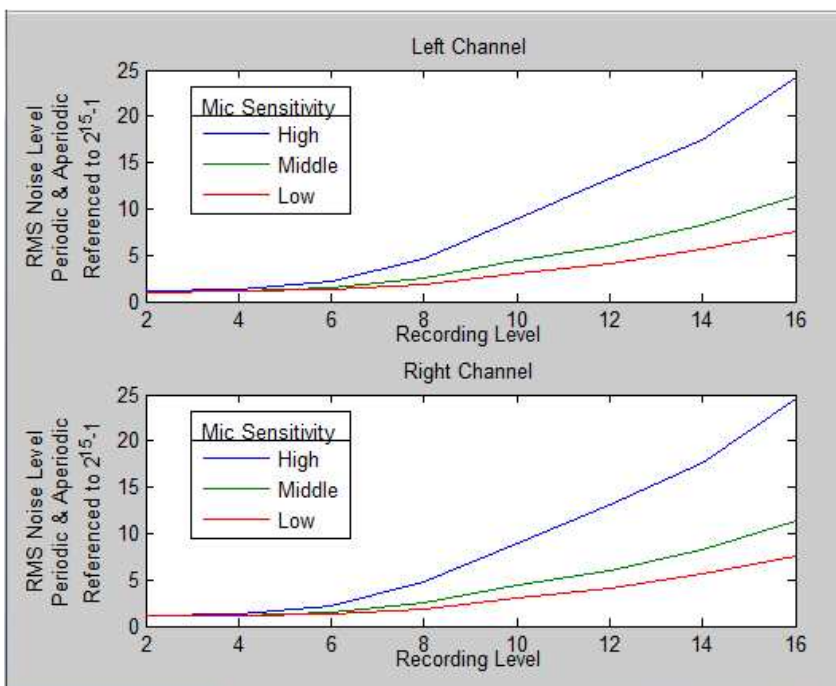


Figure A.4
DM520 – 30 Second Lab Noise Test, Fully Shielded
Shorted Input, 48k Sampling Rate, 16 Bit

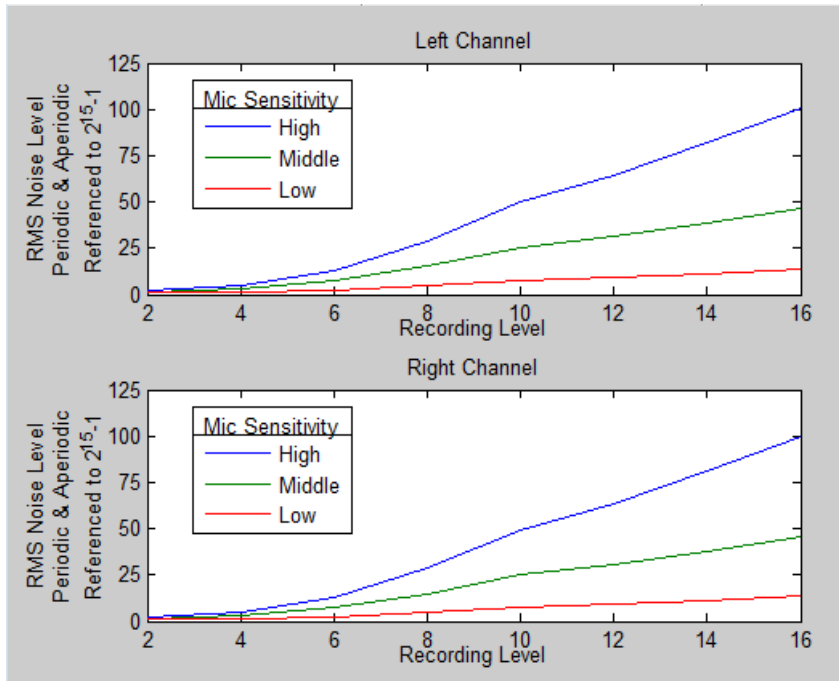


Figure A.5
DM520 – 30 Second Lab Noise Test, Fully Shielded
Open Input, 44.1k Sampling Rate, 16 Bit

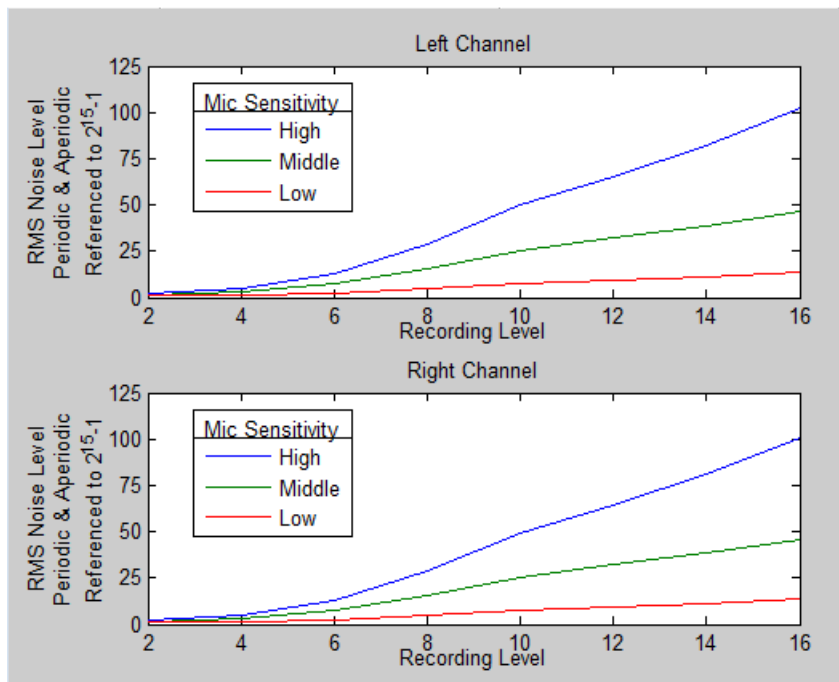


Figure A.6
DM520 – 30 Second Lab Noise Test, Fully Shielded
Open Input, 48k Sampling Rate, 16 Bit

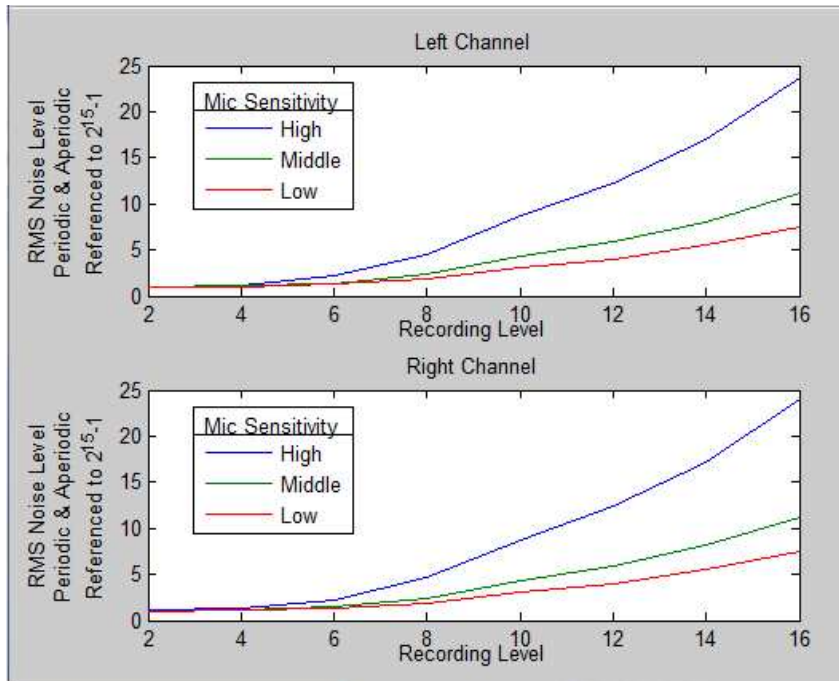


Figure A.7
 DM520 – 30 Second Lab Noise Test, Partially Shielded
 Shorted Input, 44.1k Sampling Rate, 16 Bit

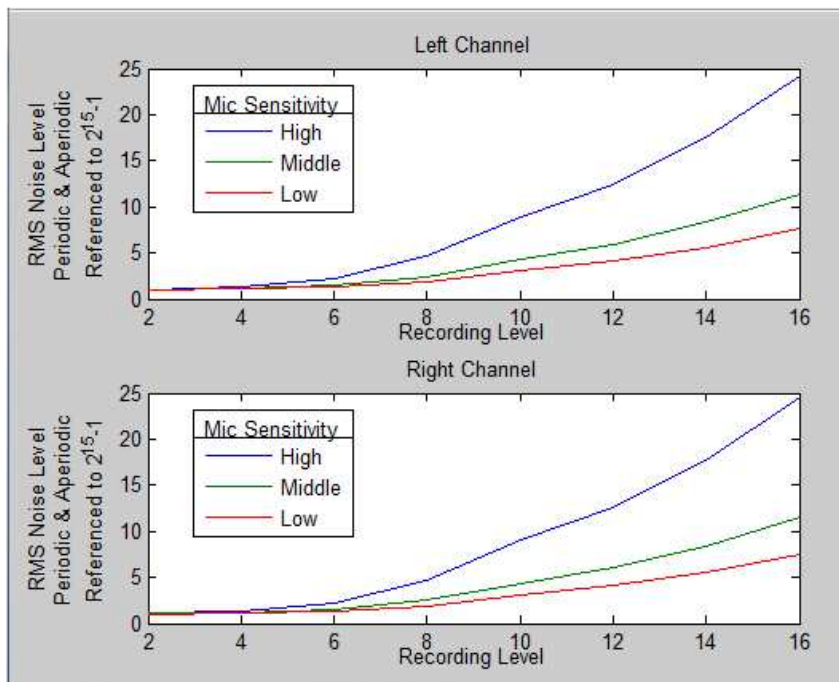


Figure A.8
 DM520 – 30 Second Lab Noise Test, Partially Shielded
 Shorted Input, 48k Sampling Rate, 16 Bit

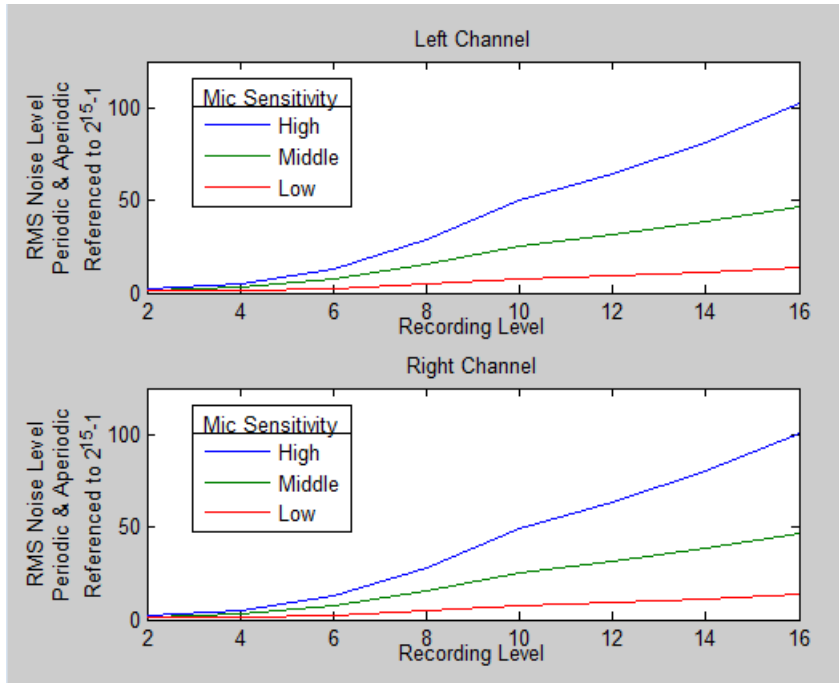


Figure A.9
DM520 – 30 Second Lab Noise Test, Partially Shielded
Open Input, 44.1k Sampling Rate, 16 Bit

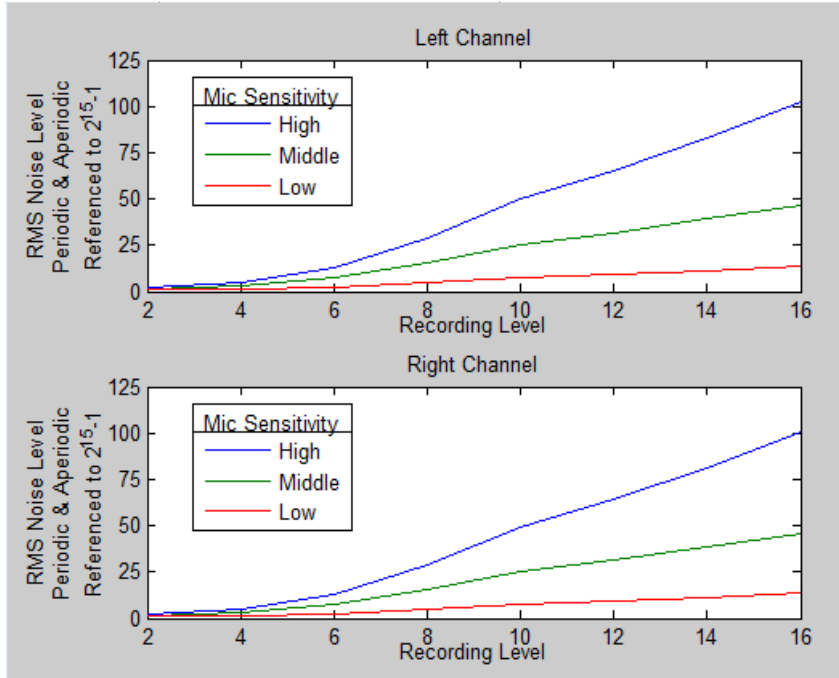


Figure A.10
DM520 – 30 Second Lab Noise Test, Partially Shielded
Open Input, 48k Sampling Rate, 16 Bit

APPENDIX B
ADDITIONAL HARMONIC LEVEL GRAPHS

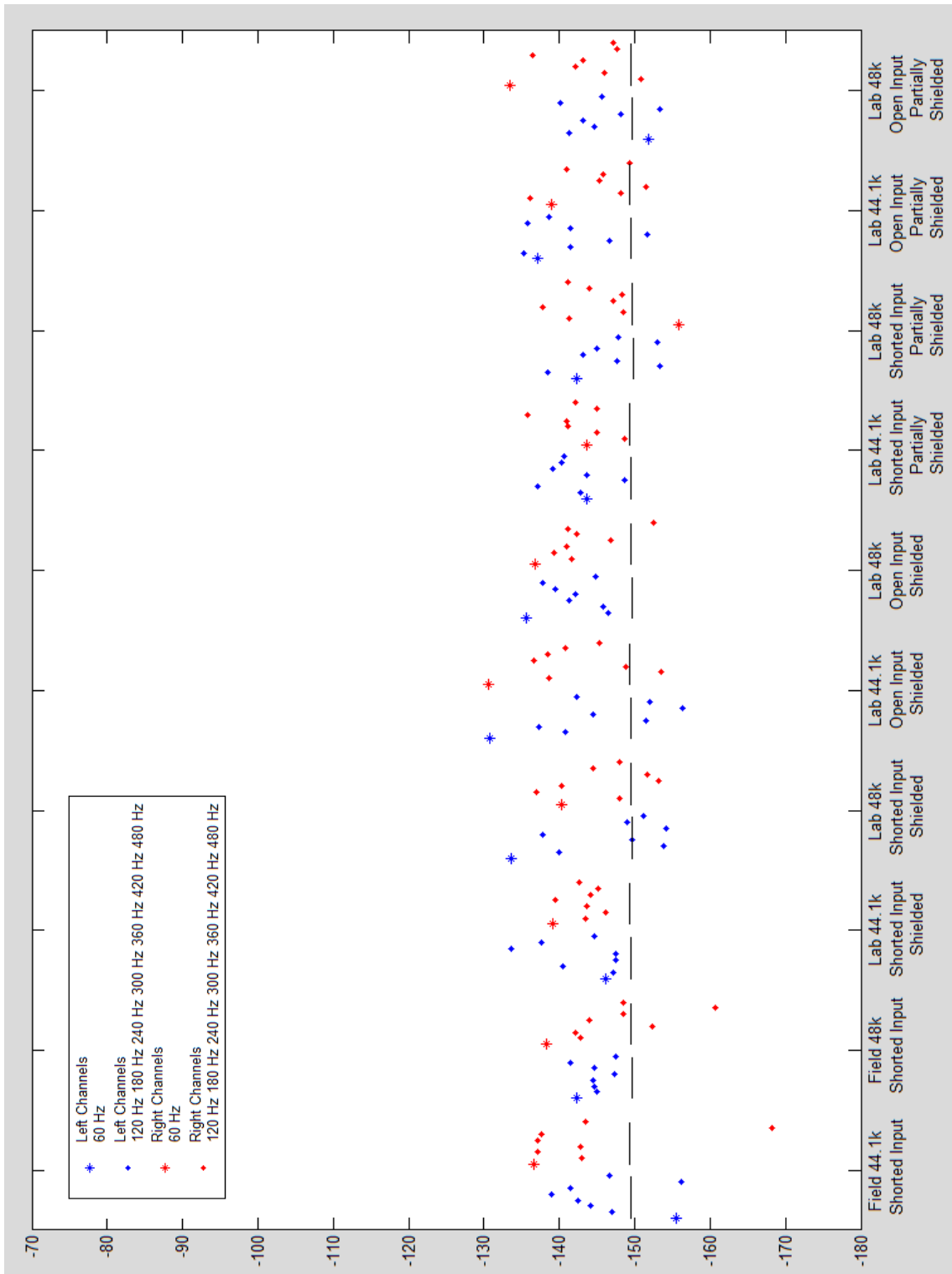


Figure B.1
DM520 – 30 Second Lab Noise Test
60 Hz Harmonic Levels
Low Microphone Sensitivity, Recording Level 2

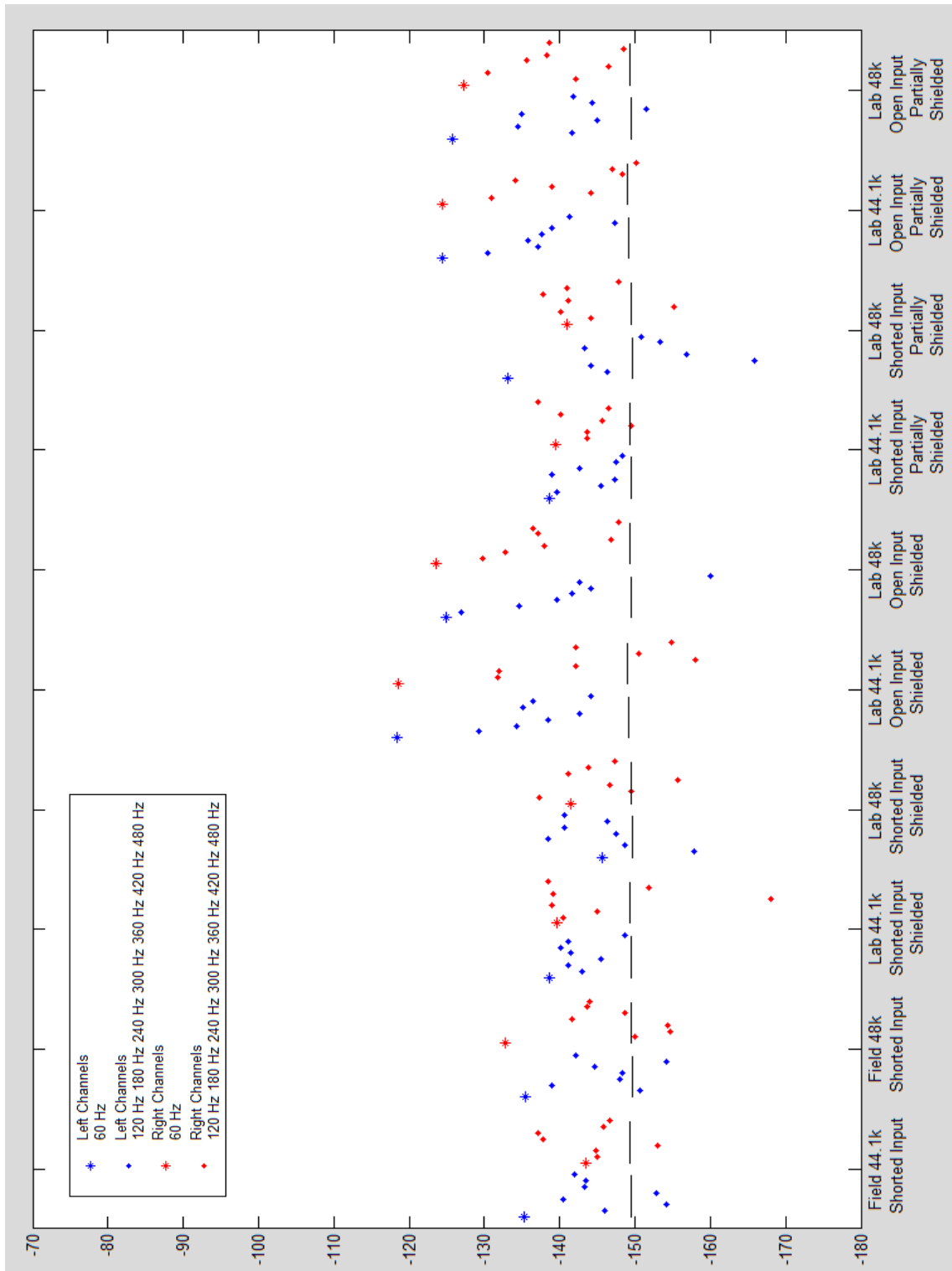


Figure B.2
DM520 – 30 Second Lab Noise Test
60 Hz Harmonic Levels
Medium Microphone Sensitivity, Recording Level 2

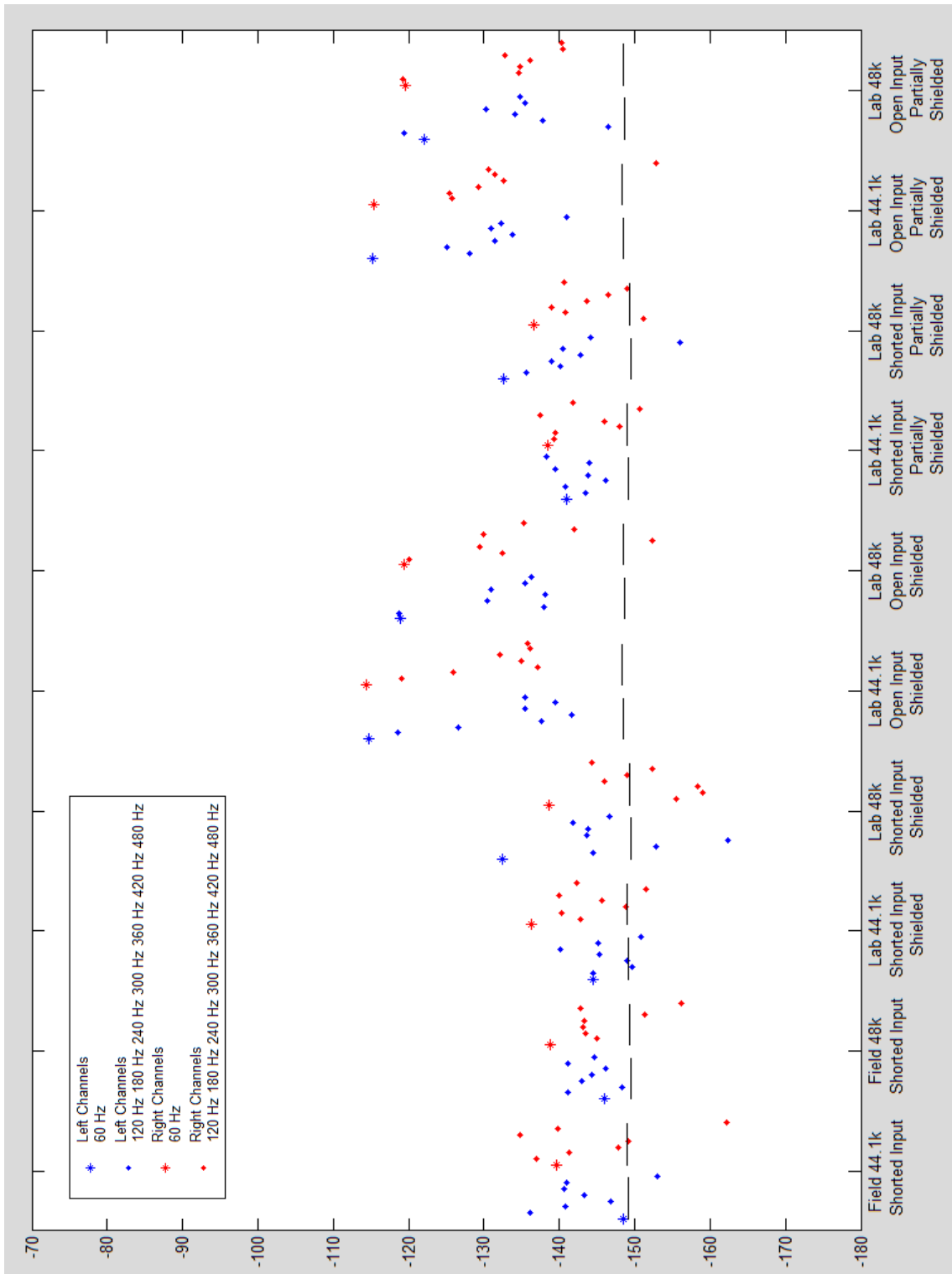


Figure B.3
DM520 – 30 Second Lab Noise Test
60 Hz Harmonic Levels
High Microphone Sensitivity, Recording Level 2

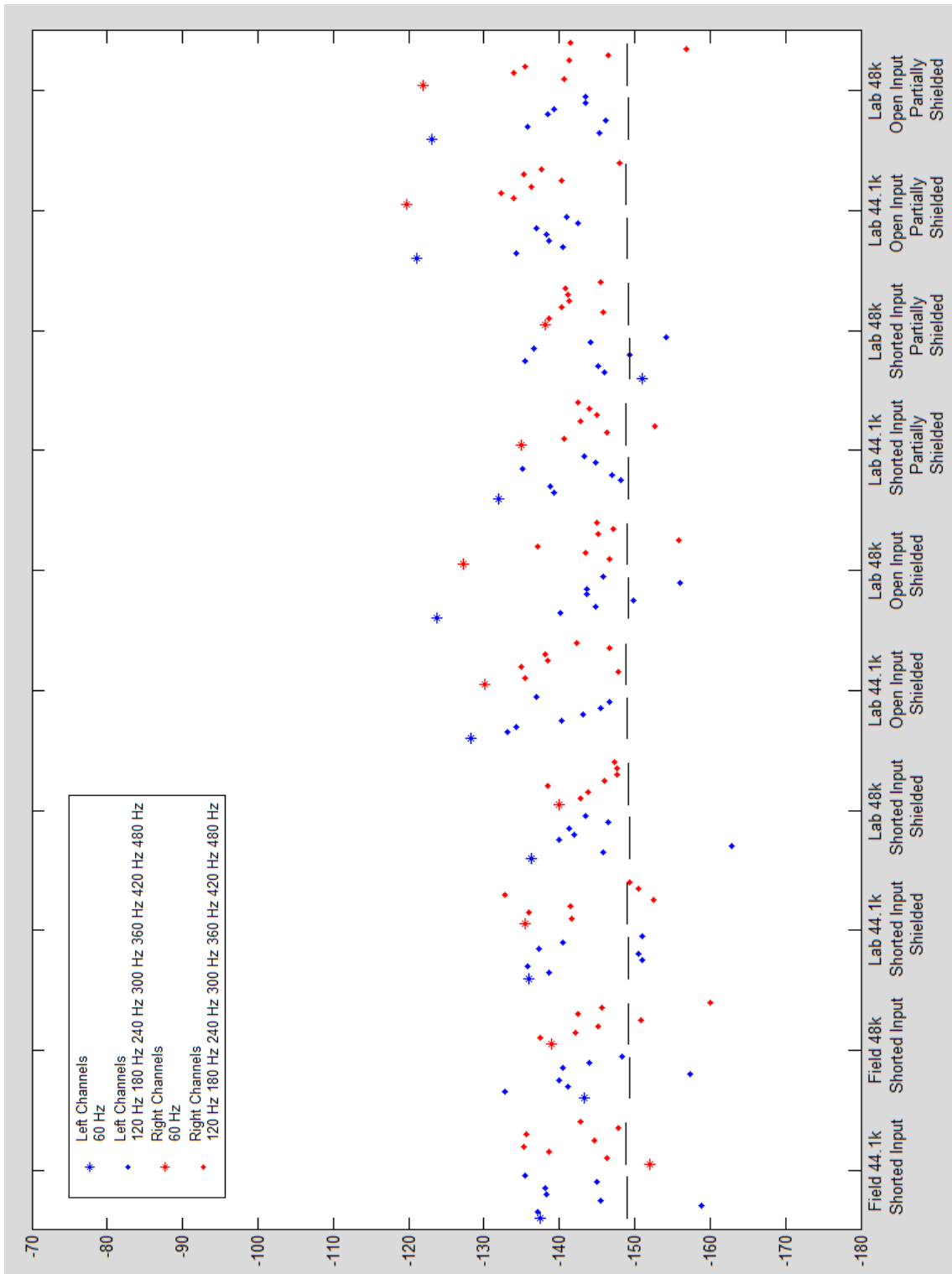


Figure B.4
DM520 – 30 Second Lab Noise Test
60 Hz Harmonic Levels
Low Microphone Sensitivity, Recording Level 4

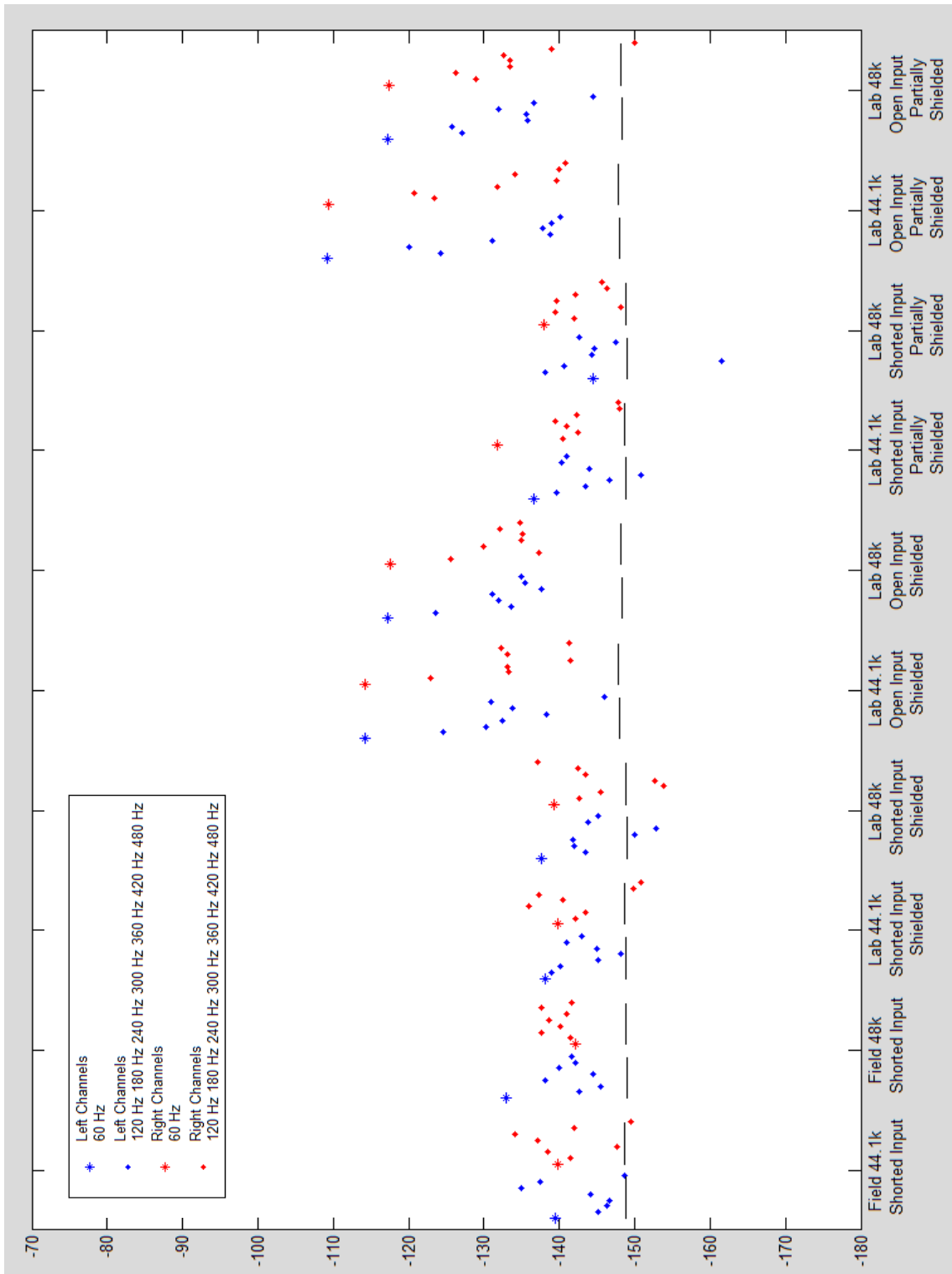


Figure B.5
DM520 – 30 Second Lab Noise Test
60 Hz Harmonic Levels
Medium Microphone Sensitivity, Recording Level 4

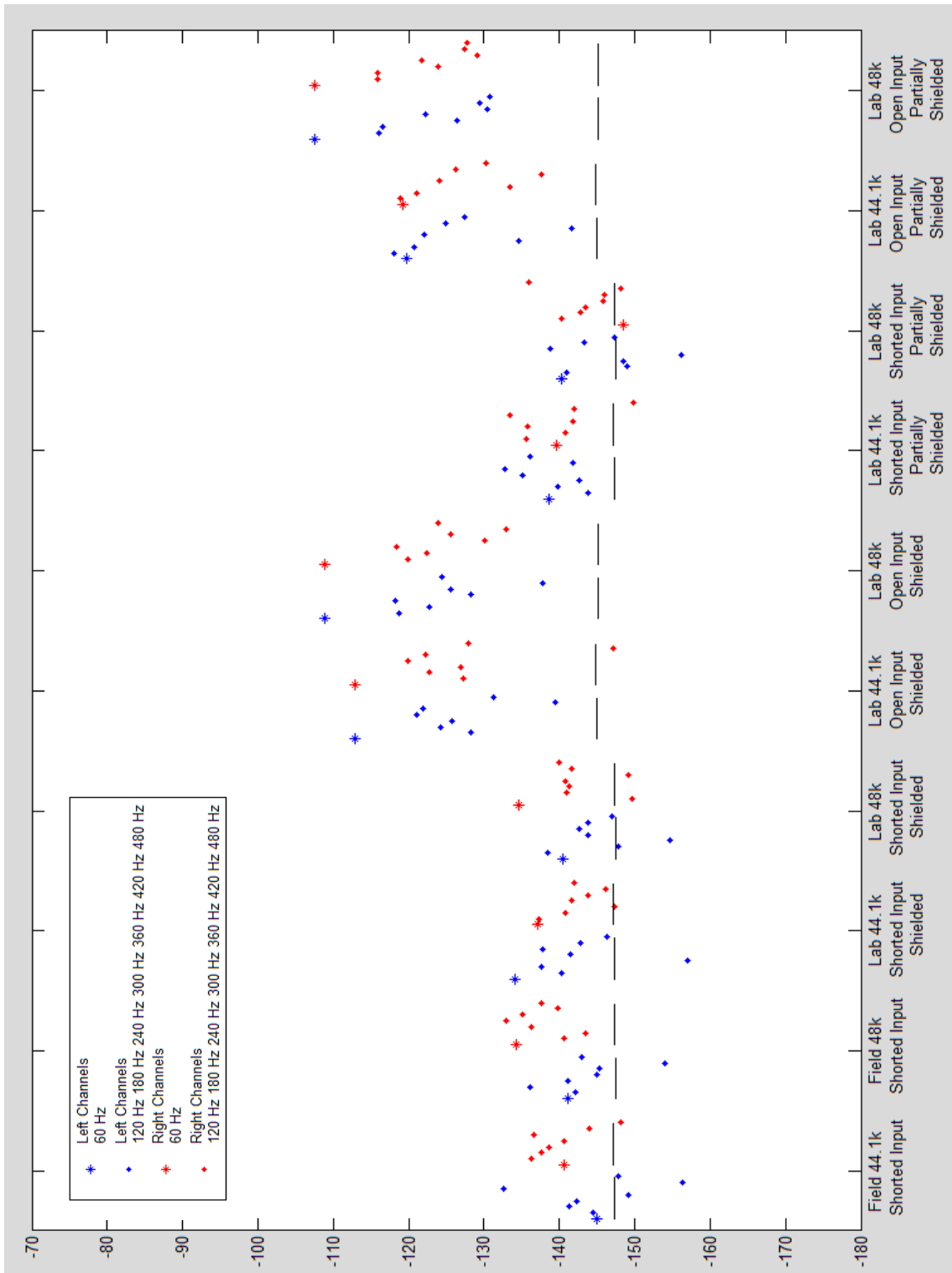


Figure B.6
DM520 – 30 Second Lab Noise Test
60 Hz Harmonic Levels
High Microphone Sensitivity, Recording Level 4

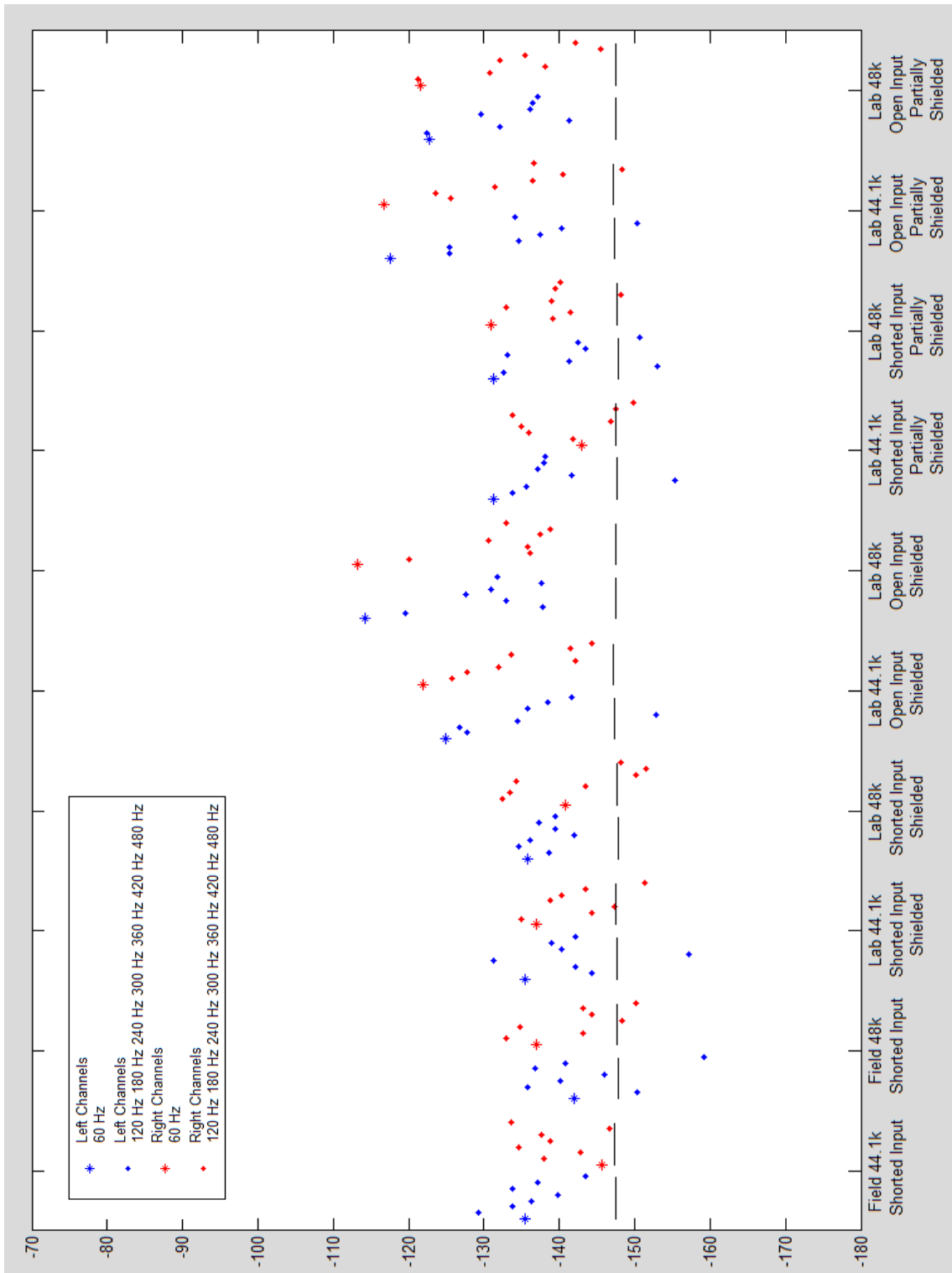


Figure B.7
DM520 – 30 Second Lab Noise Test
60 Hz Harmonic Levels
Low Microphone Sensitivity, Recording Level 6

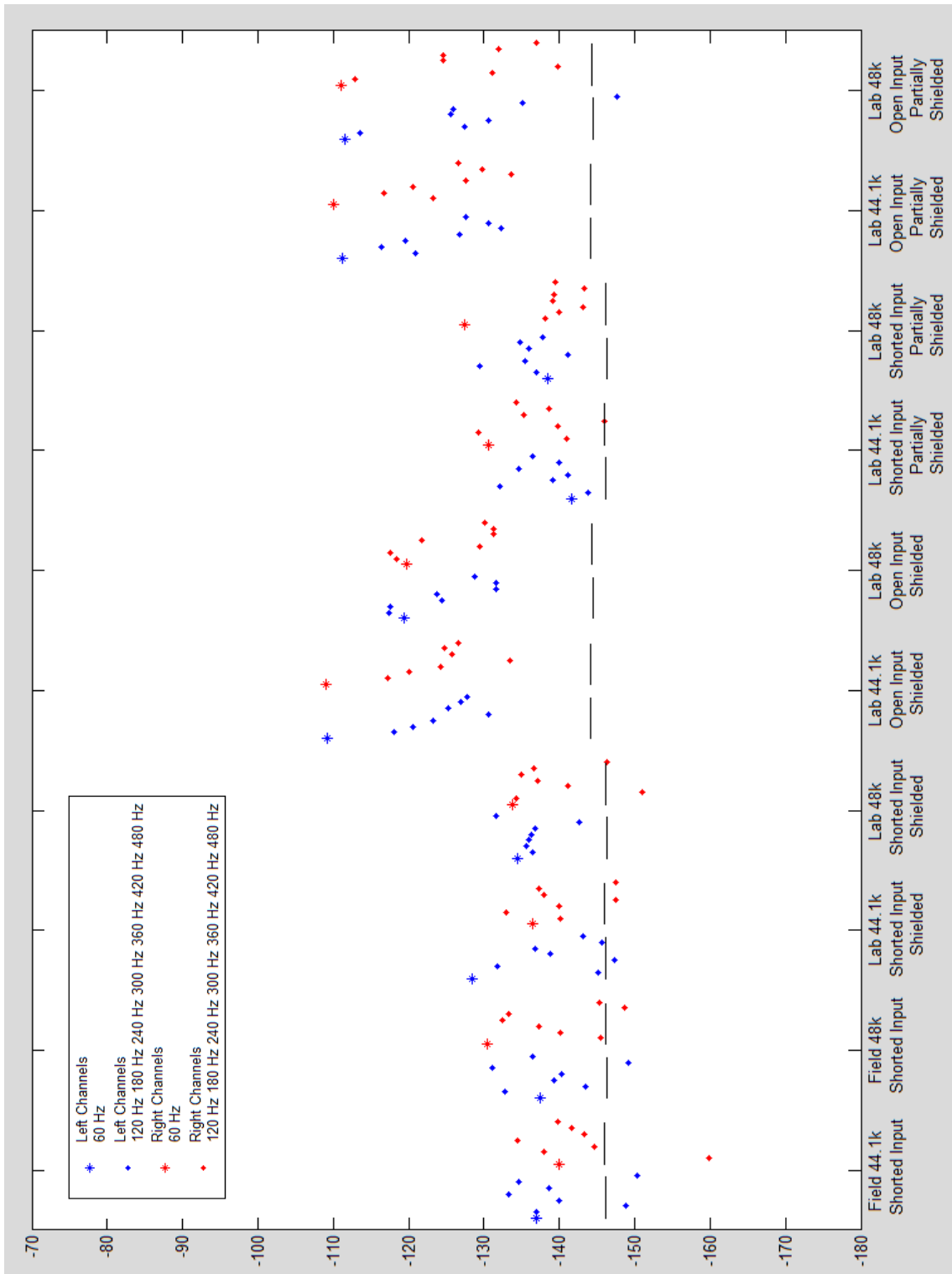


Figure B.8
DM520 – 30 Second Lab Noise Test
60 Hz Harmonic Levels
Medium Microphone Sensitivity, Recording Level 6

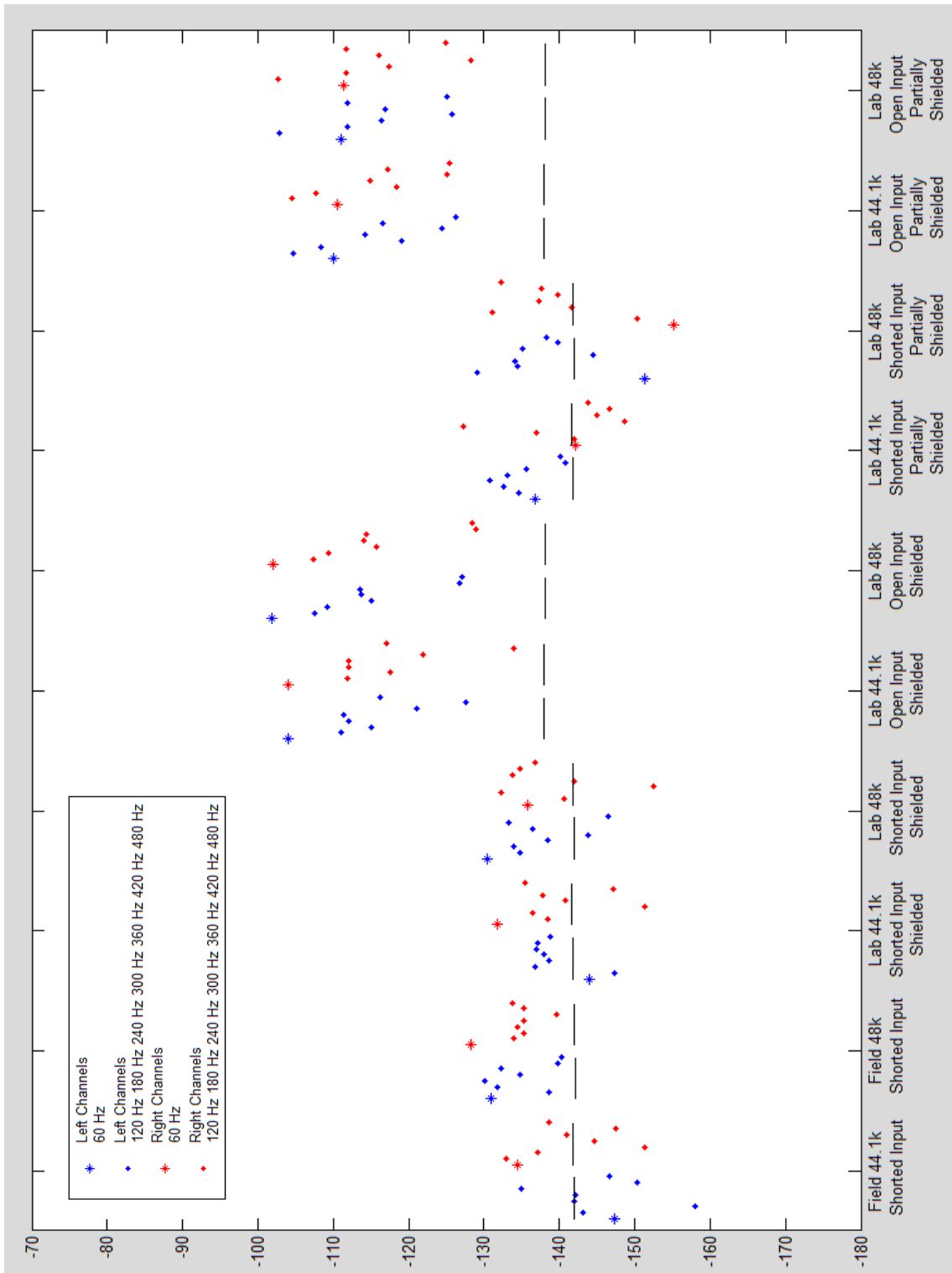


Figure B.9
DM520 – 30 Second Lab Noise Test
60 Hz Harmonic Levels
High Microphone Sensitivity, Recording Level 6

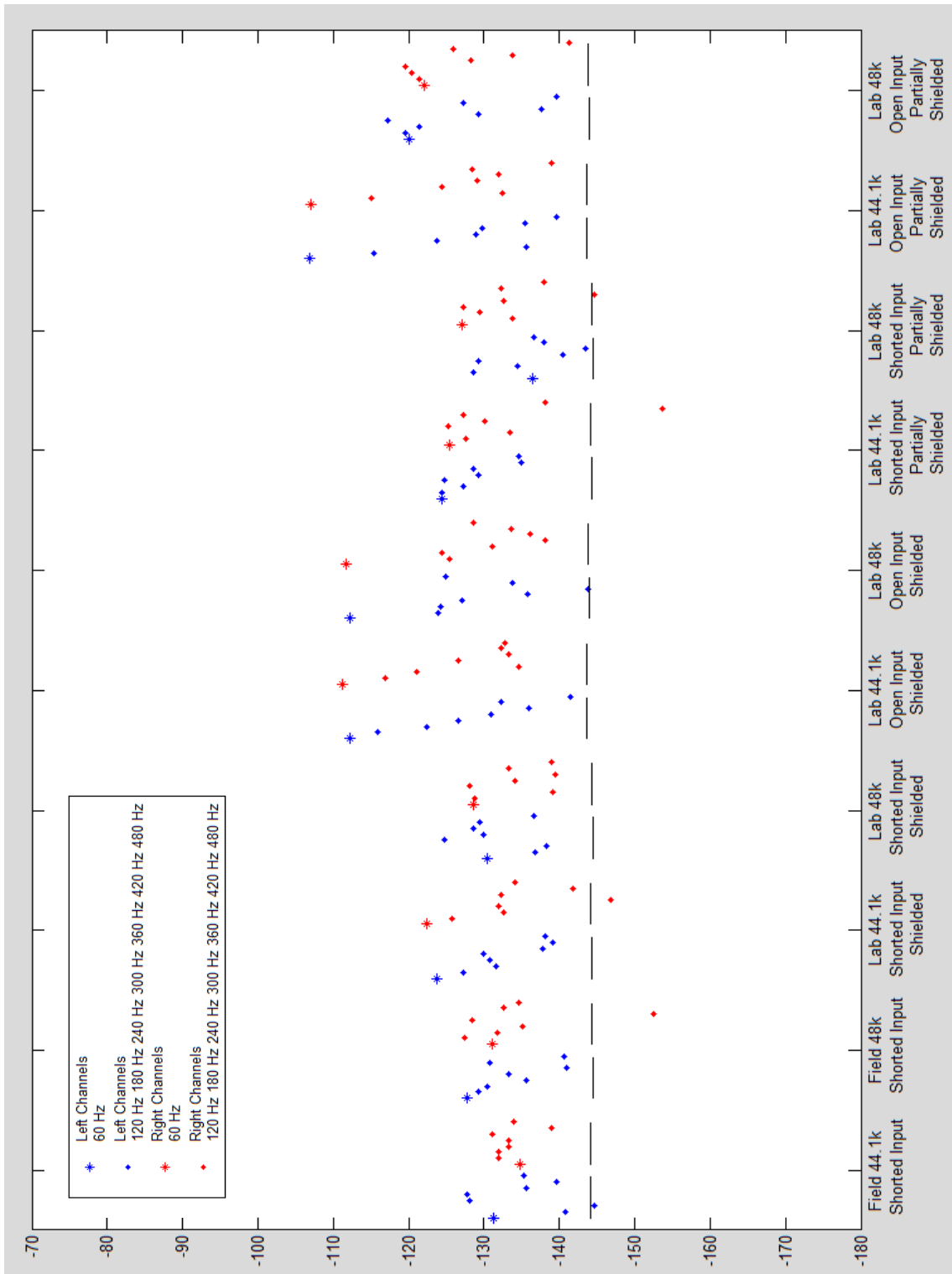


Figure B.10
DM520 – 30 Second Lab Noise Test
60 Hz Harmonic Levels
Low Microphone Sensitivity, Recording Level 8

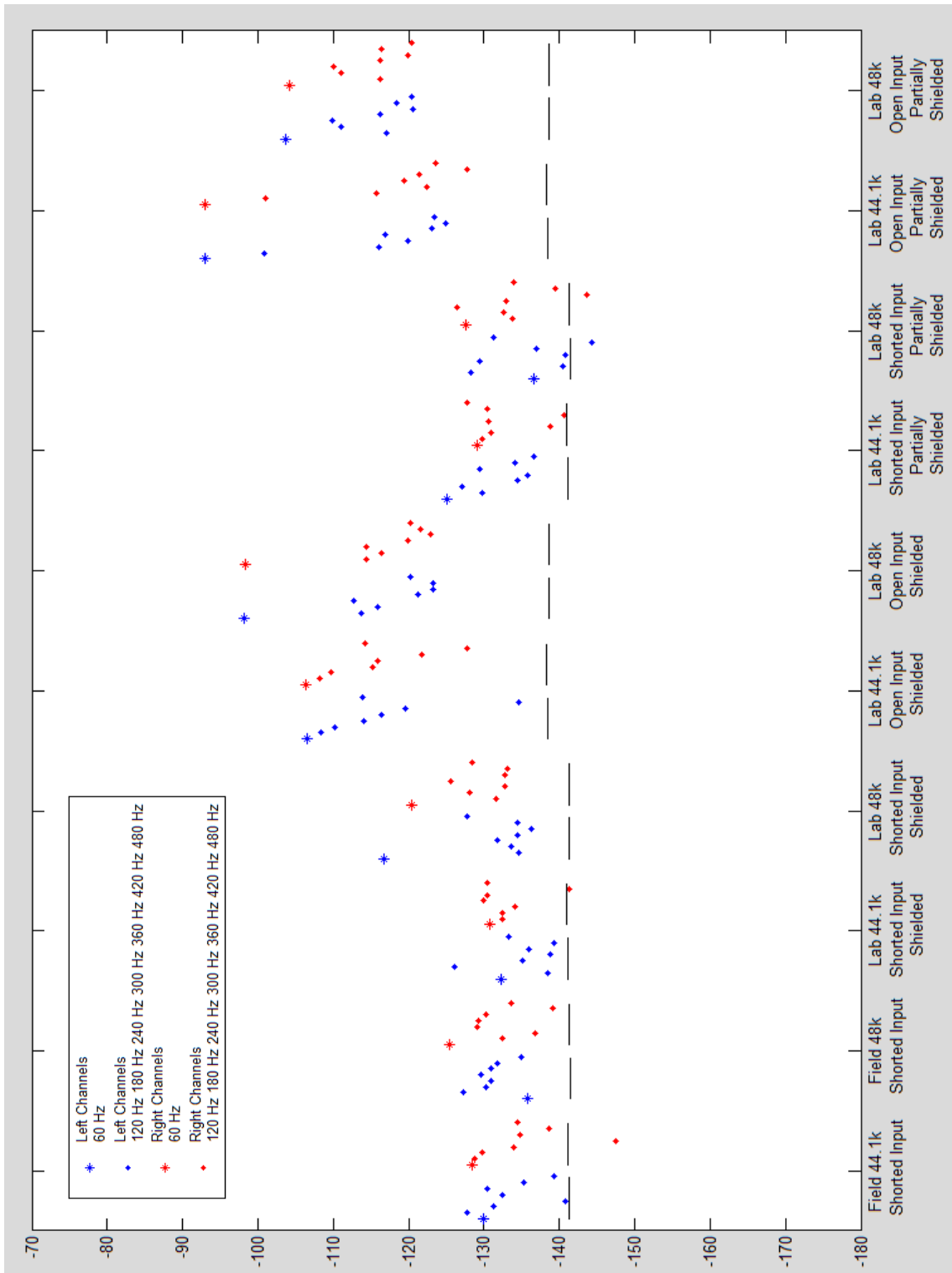


Figure B.11
DM520 – 30 Second Lab Noise Test
60 Hz Harmonic Levels
Medium Microphone Sensitivity, Recording Level 8

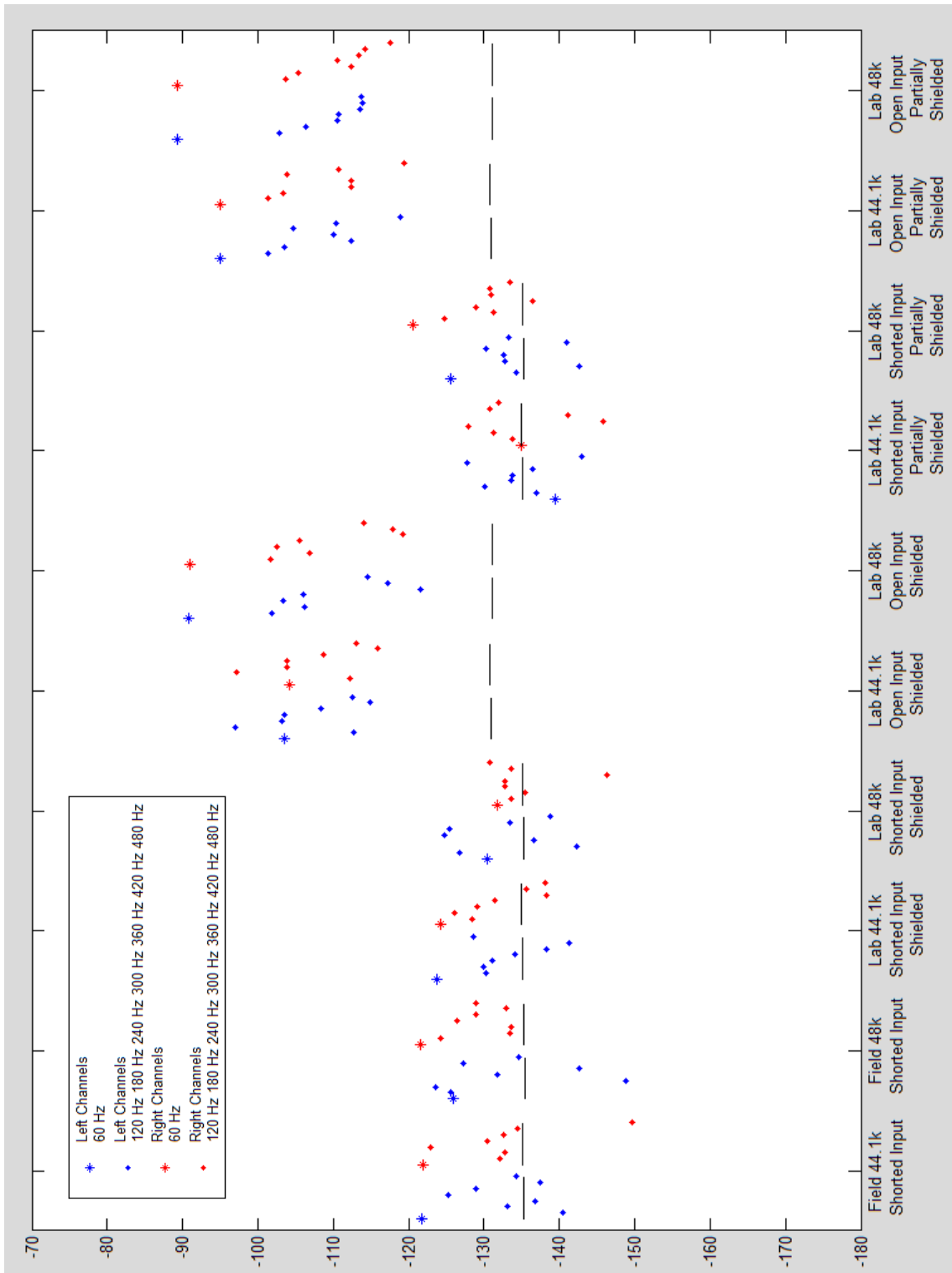


Figure B.12
DM520 – 30 Second Lab Noise Test
60 Hz Harmonic Levels
High Microphone Sensitivity, Recording Level 8

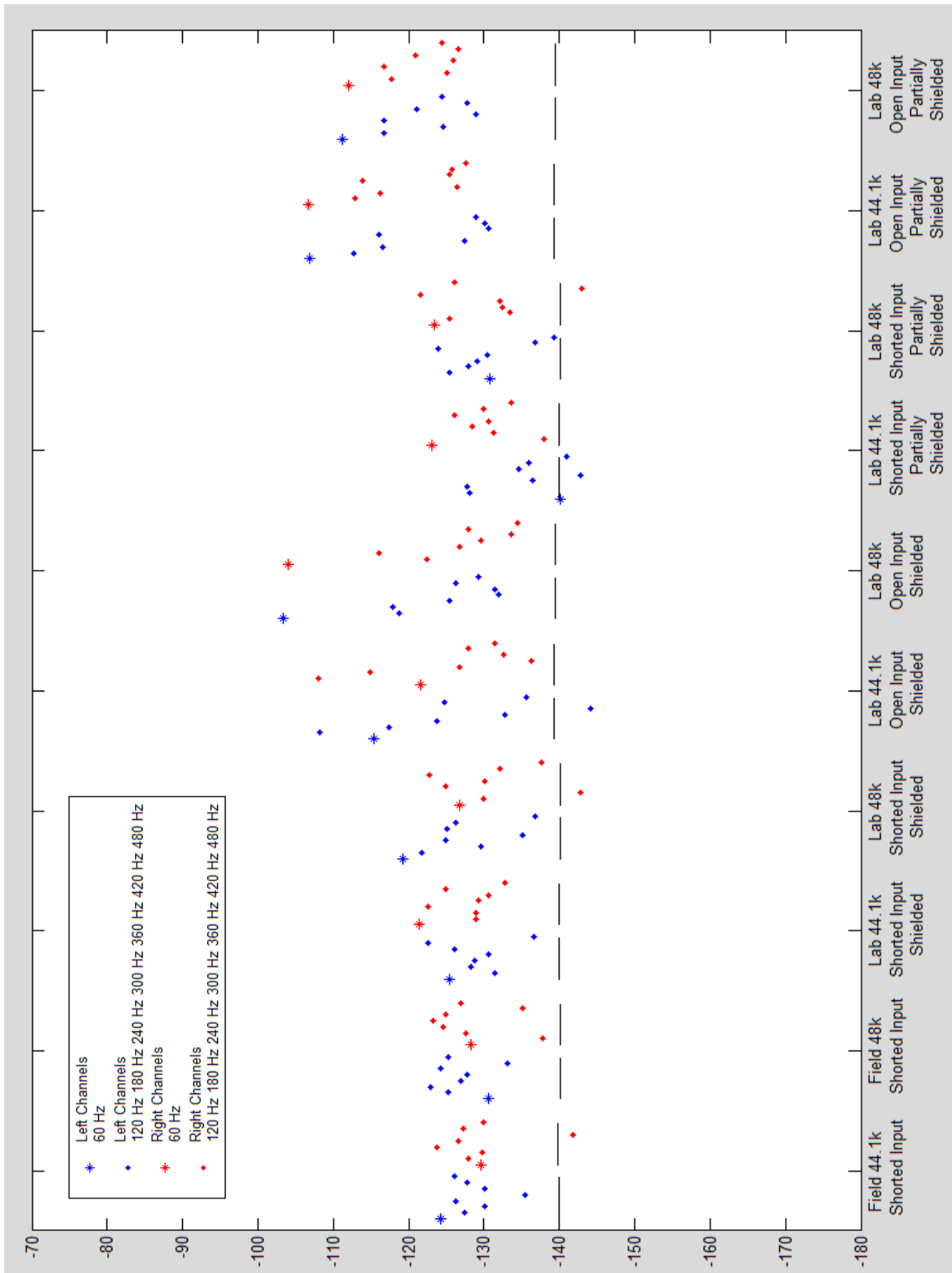


Figure B.13
DM520 – 30 Second Lab Noise Test
60 Hz Harmonic Levels
Low Microphone Sensitivity, Recording Level 10

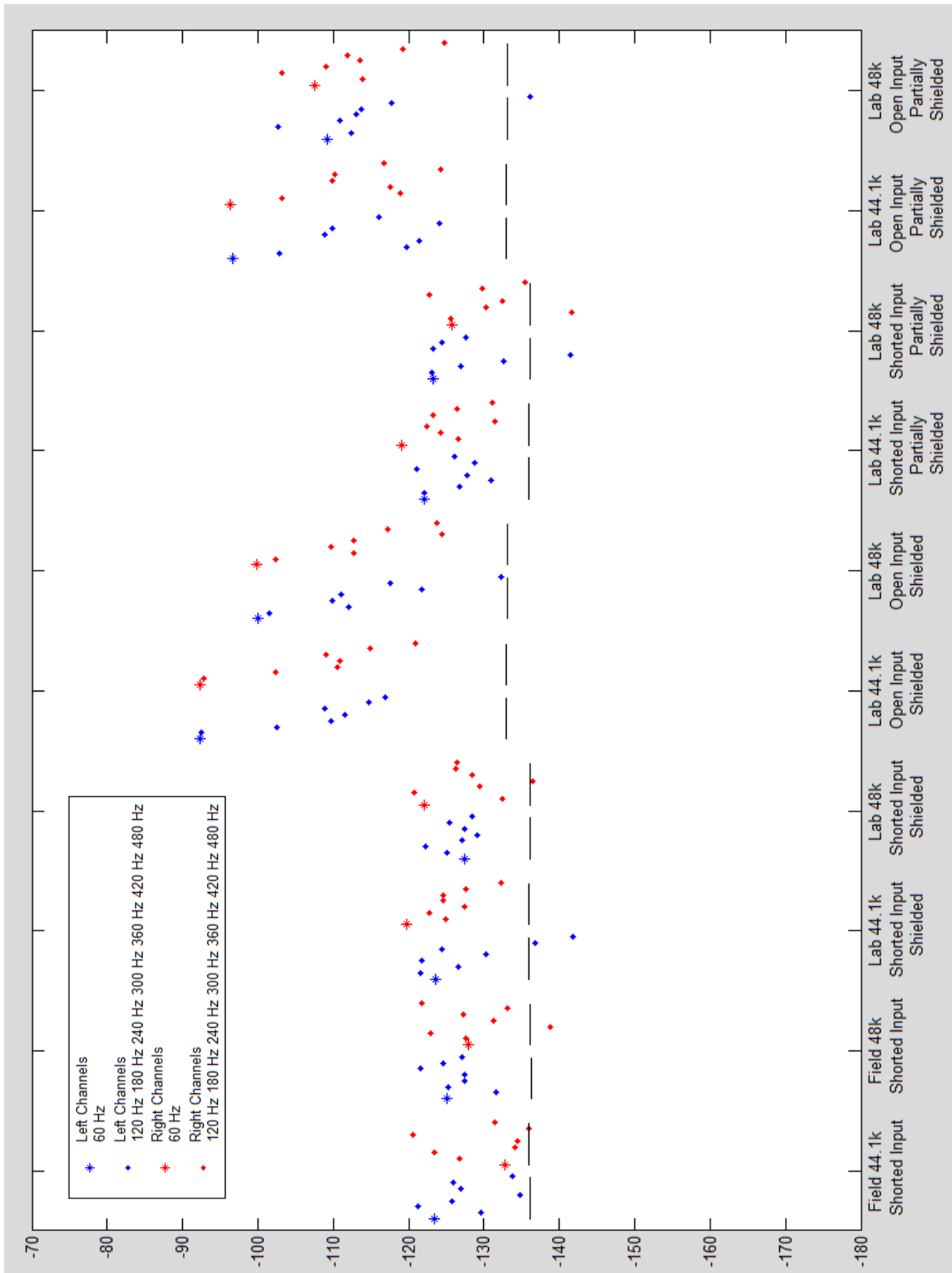


Figure B.14
DM520 – 30 Second Lab Noise Test
60 Hz Harmonic Levels
Medium Microphone Sensitivity, Recording Level 10

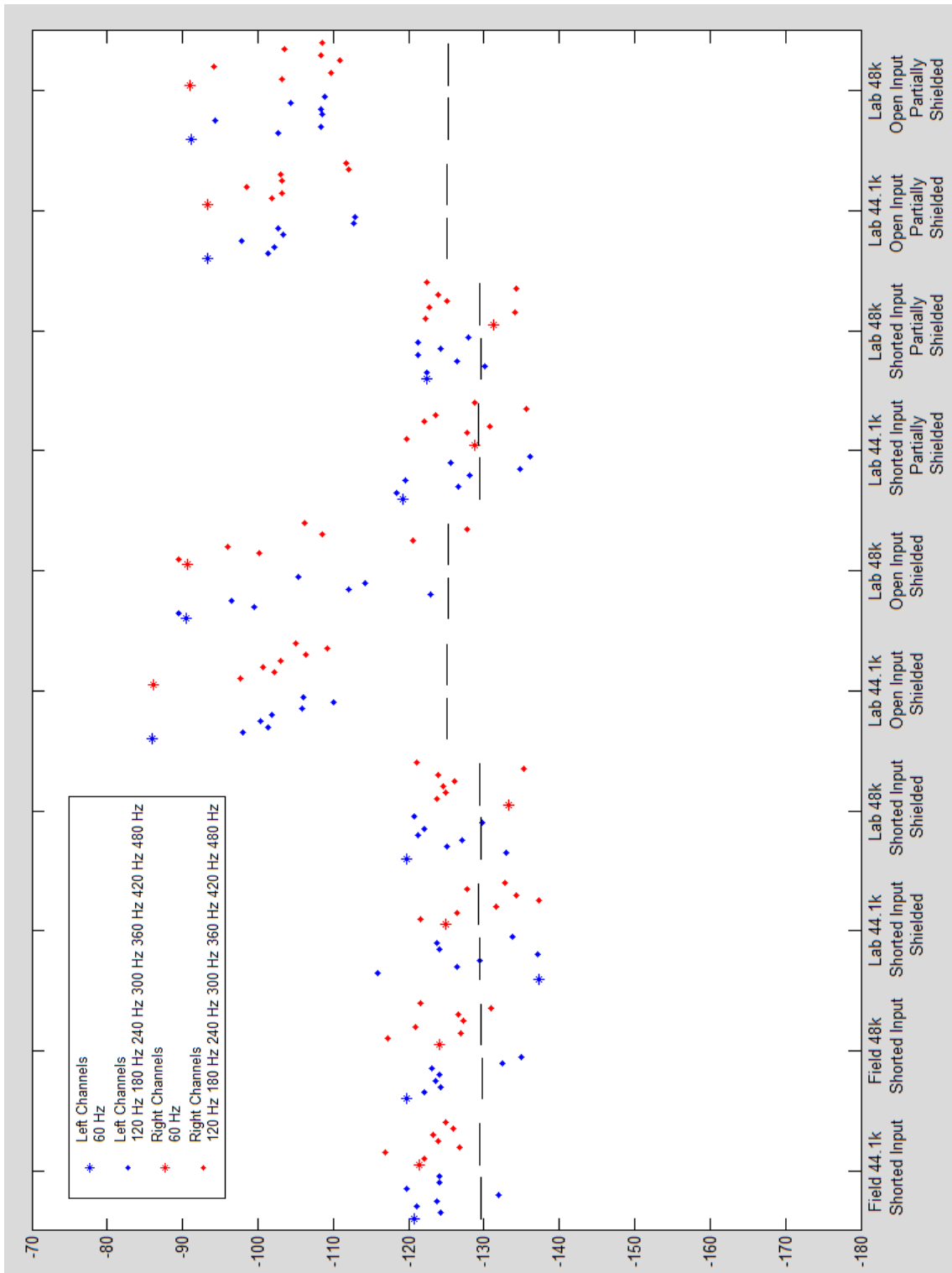


Figure B.15
DM520 – 30 Second Lab Noise Test
60 Hz Harmonic Levels
High Microphone Sensitivity, Recording Level 10

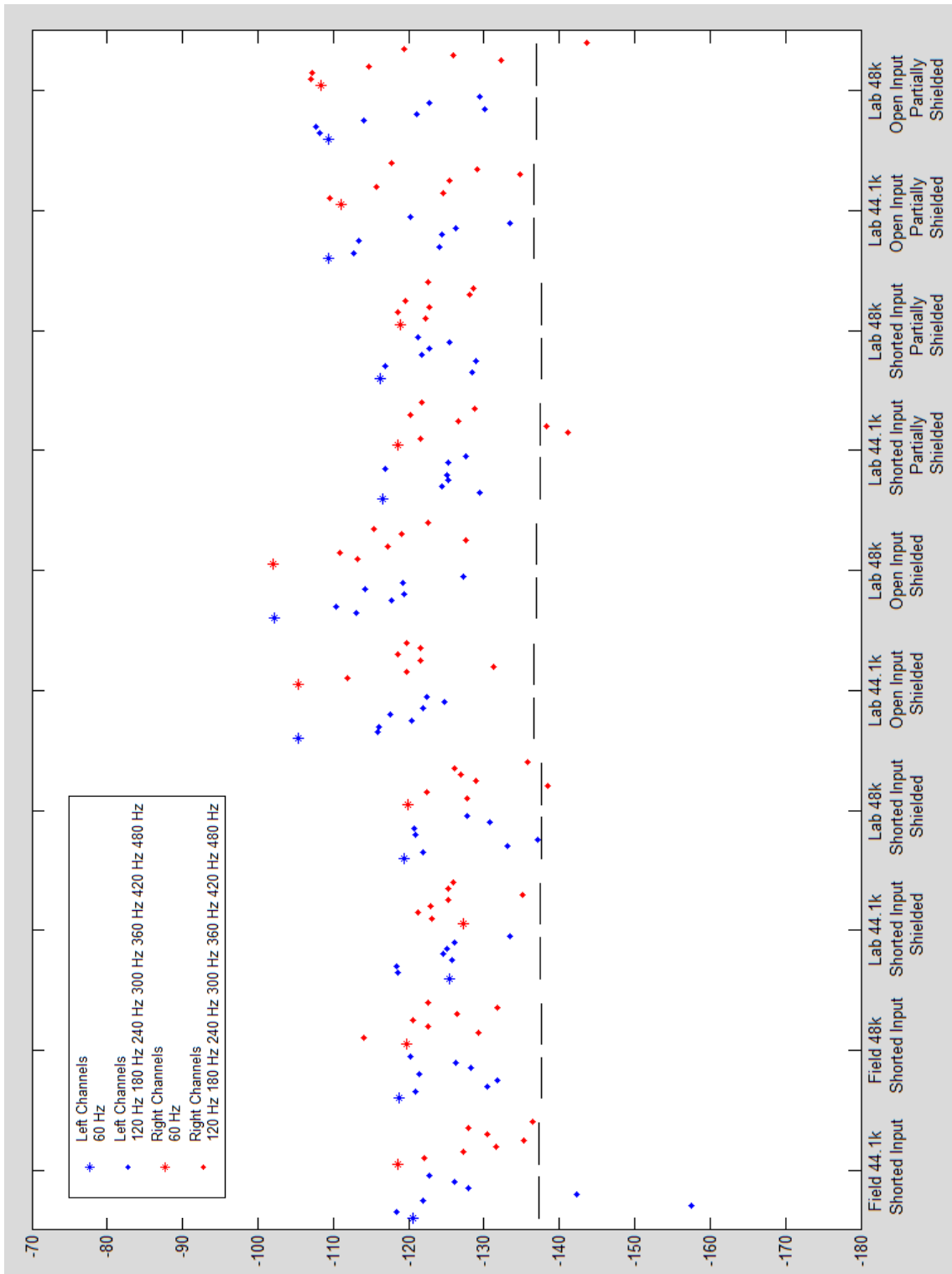


Figure B.16
DM520 – 30 Second Lab Noise Test
60 Hz Harmonic Levels
Low Microphone Sensitivity, Recording Level 12

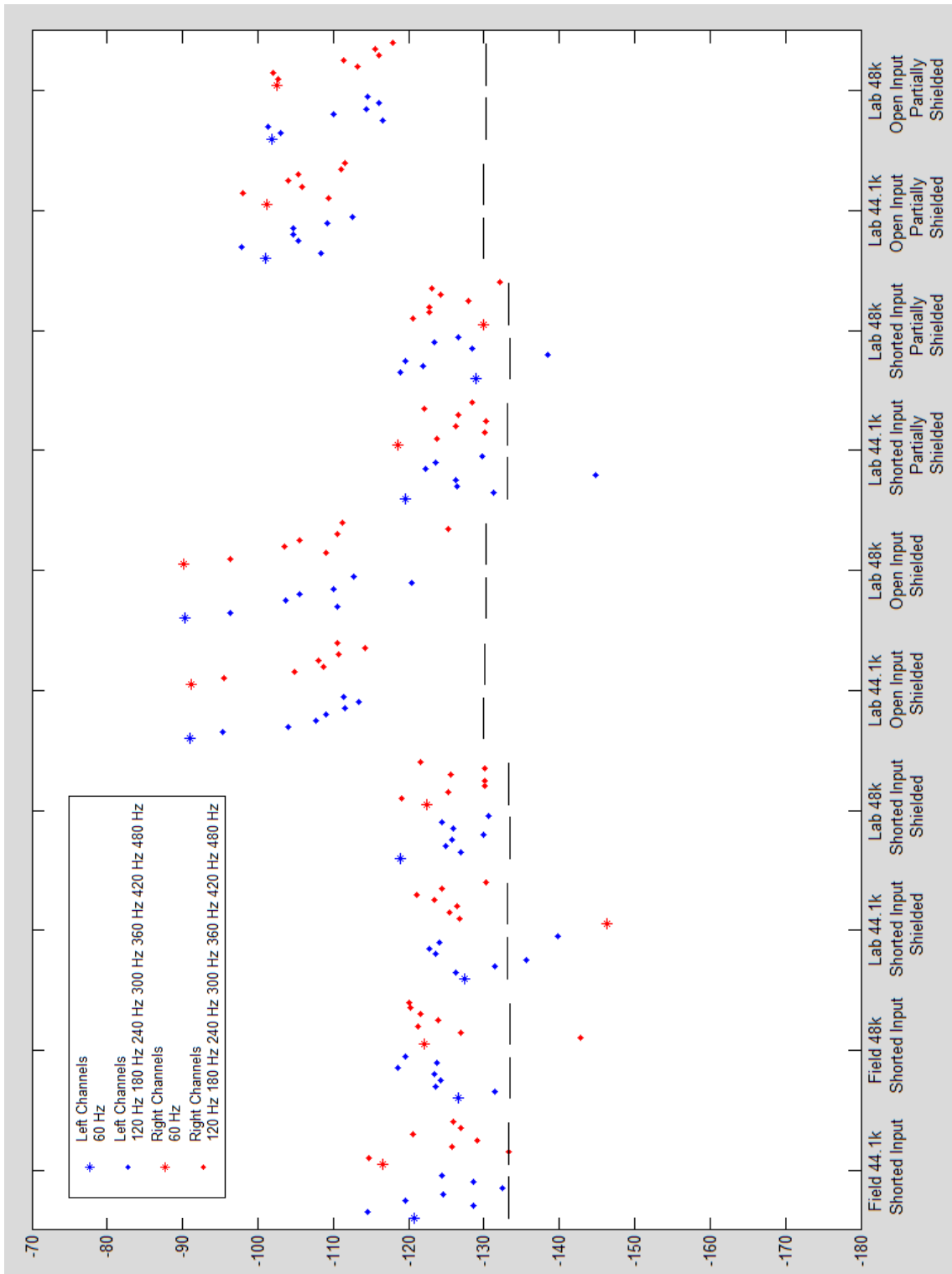


Figure B.17
DM520 – 30 Second Lab Noise Test
60 Hz Harmonic Levels
Medium Microphone Sensitivity, Recording Level 12

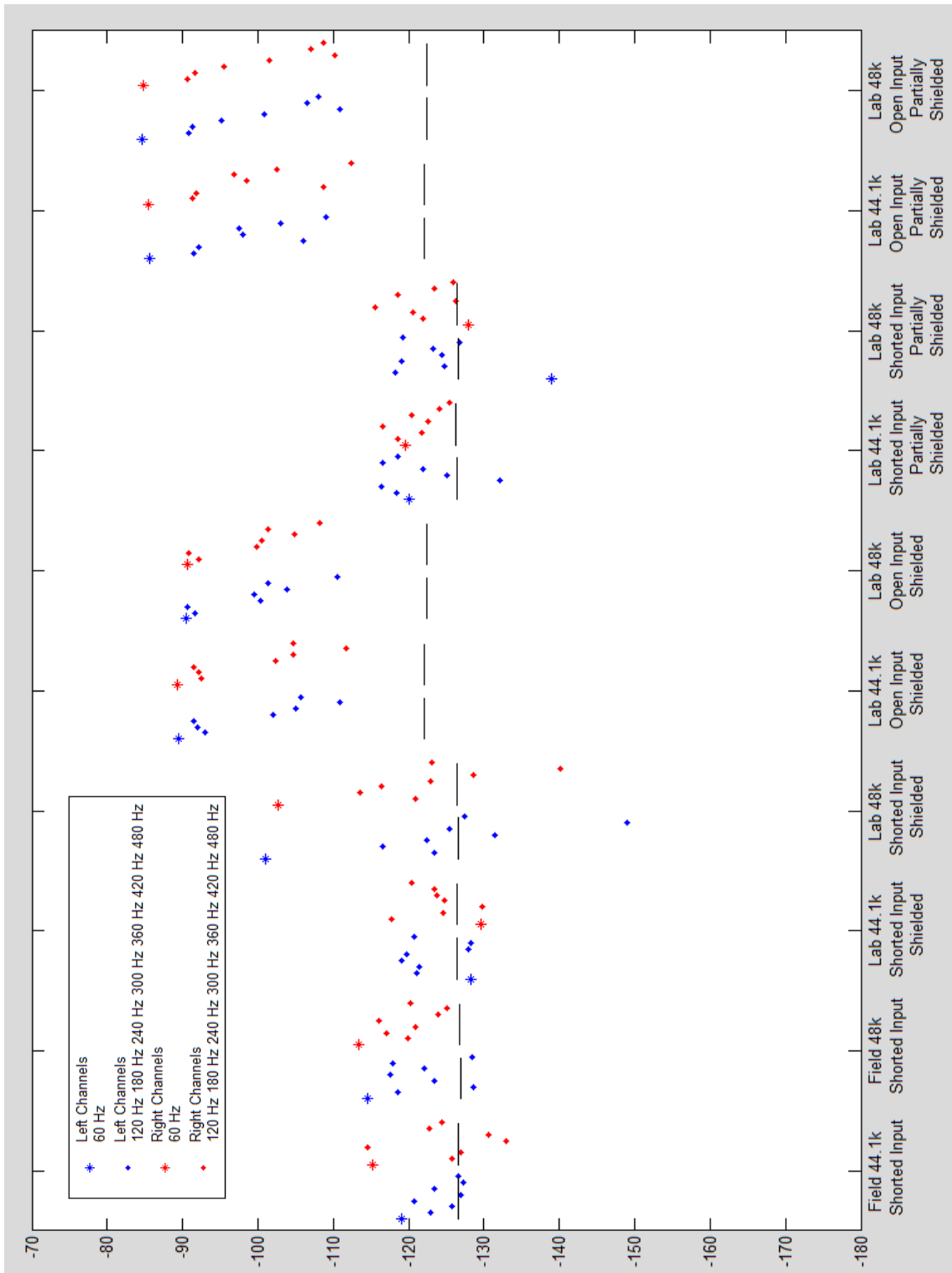


Figure B.18
DM520 – 30 Second Lab Noise Test
60 Hz Harmonic Levels
High Microphone Sensitivity, Recording Level 12

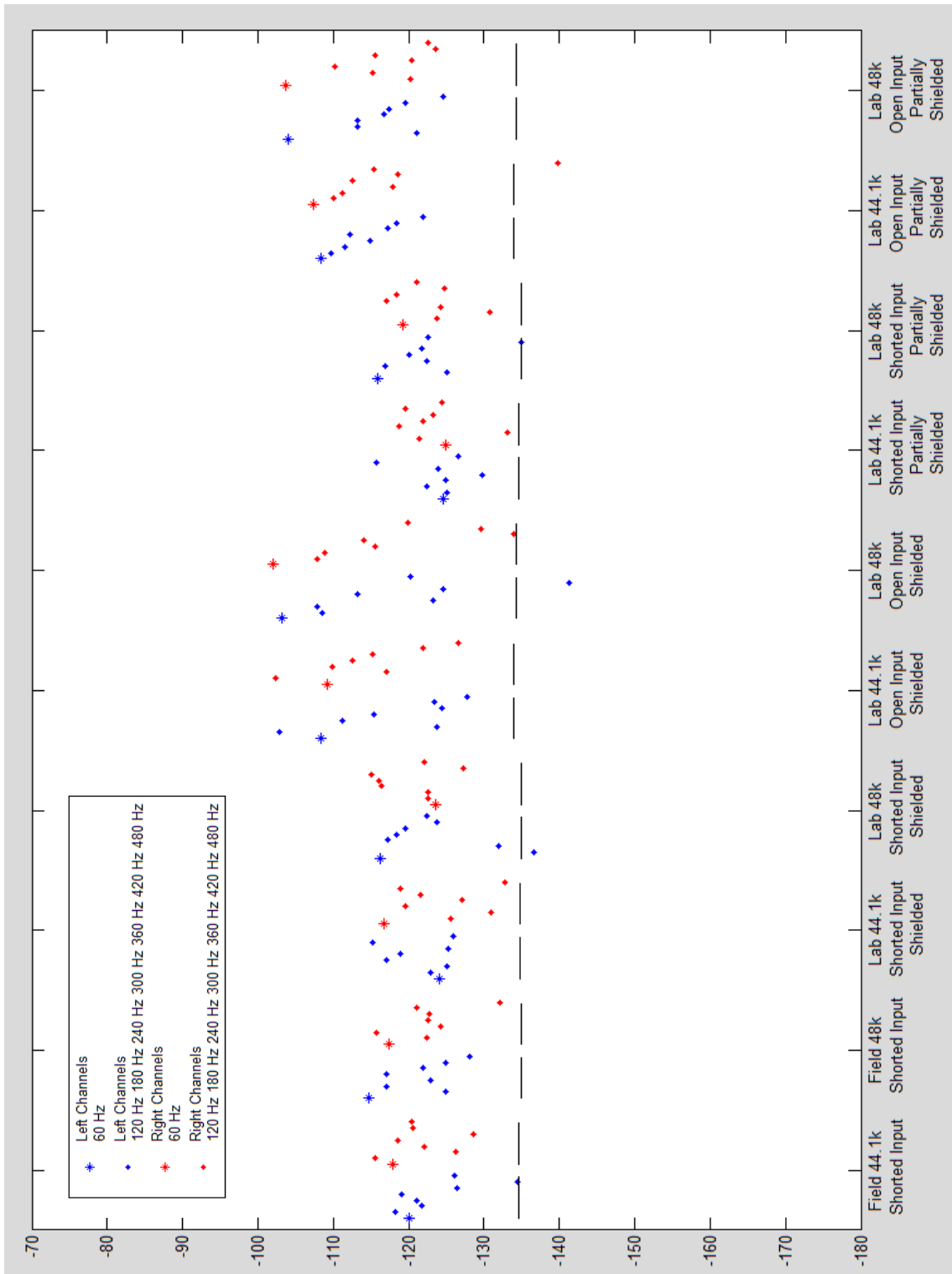


Figure B.19
DM520 – 30 Second Lab Noise Test
60 Hz Harmonic Levels
Low Microphone Sensitivity, Recording Level 14

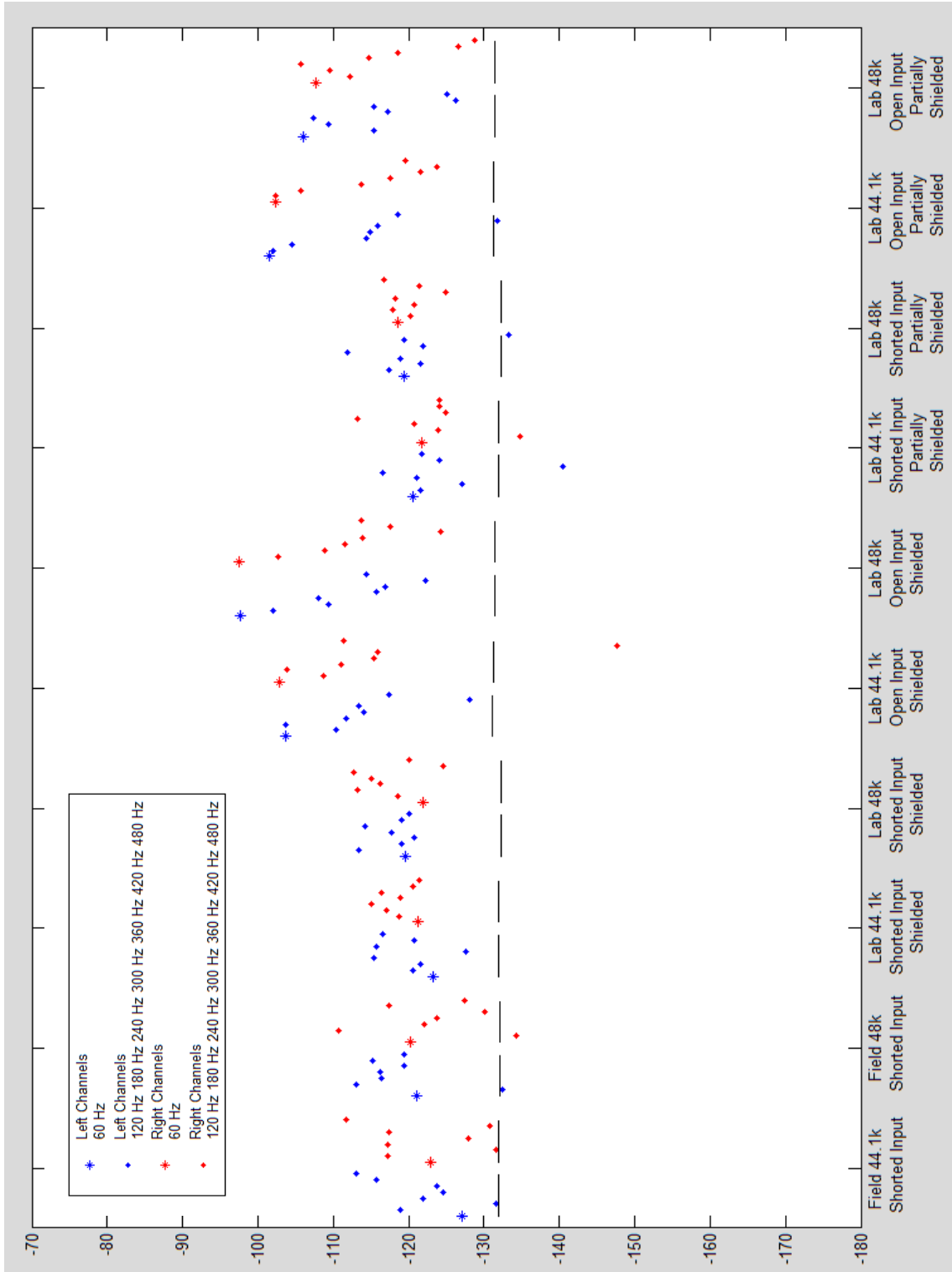


Figure B.22
DM520 – 30 Second Lab Noise Test
60 Hz Harmonic Levels
Low Microphone Sensitivity, Recording Level 16

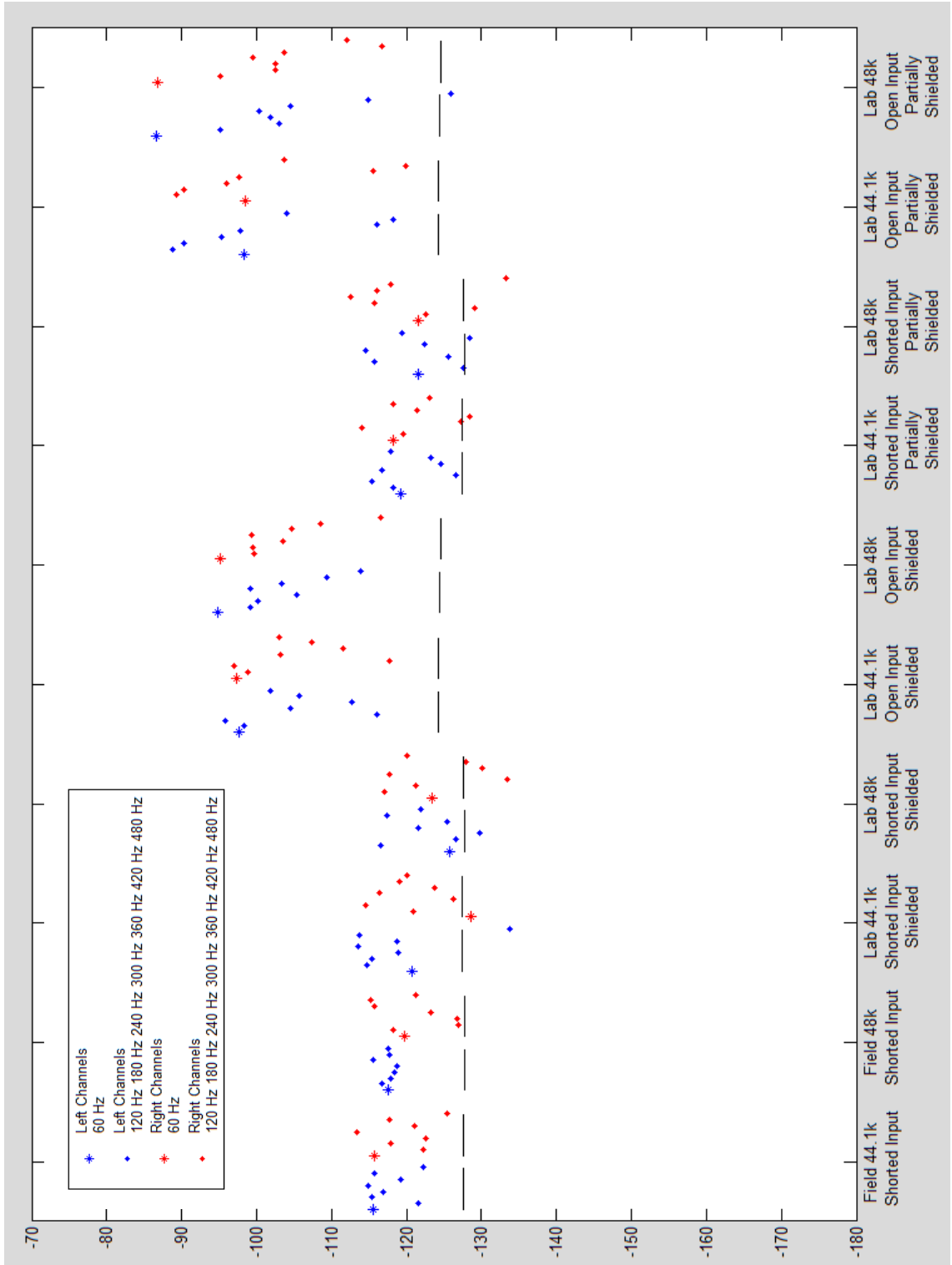


Figure B.23
DM520 – 30 Second Lab Noise Test
60 Hz Harmonic Levels
Medium Microphone Sensitivity, Recording Level 16

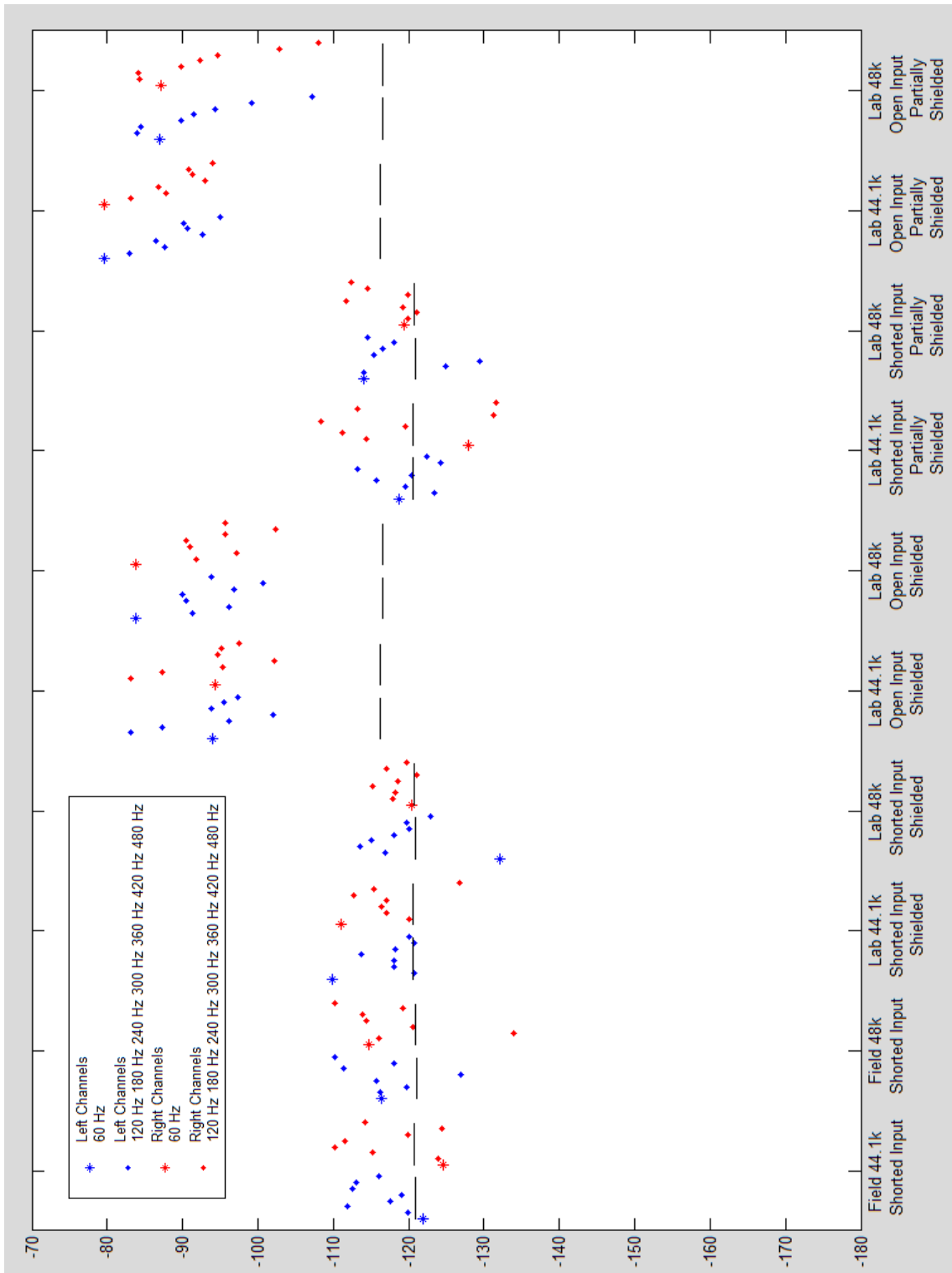


Figure B.24
DM520 – 30 Second Lab Noise Test
60 Hz Harmonic Levels
High Microphone Sensitivity, Recording Level 16

APPENDIX C

EQUATIONS

For

M : Mean Amplitude
 S : Sampling Rate
 A : Bin Amplitude
 n : Bin Number

Where

$$n \rightarrow \infty \text{ as } S \rightarrow \infty$$

Then

$$\lim_{S \rightarrow \infty} \frac{\sum_{n=2}^{\frac{S}{2}} A_n}{\frac{S}{2} - 1} = 0$$

And

$$M = \frac{\sum_{n=2}^{\frac{S}{2}} A_n}{\frac{S}{2} - 1}$$